Inhibition of DNA replication by an anti-PCNA aptamer/PCNA complex

Ewa Kowalska[1], Filip Bartnicki[1], Ryo Fujisawa[2], Piotr Bonarek[3], Paweł Hermanowicz[1,4], Toshiki Tsurimoto[2], Klaudia Muszyńska[1] and Wojciech Strzalka[1,*]

[1]Department of Plant Biotechnology, Faculty of Biochemistry, Biophysics and Biotechnology, Jagiellonian University, Gronostajowa 7, Krakow 30-387, Poland, [2]Department of Biology, Faculty of Science, Kyushu University, 744 Motooka, Nishi-ku, Fukuoka 819-0395, Japan, [3]Department of Physical Biochemistry, Faculty of Biochemistry, Biophysics and Biotechnology, Jagiellonian University, Gronostajowa 7, Krakow 30-387, Poland and [4]Laboratory of Photobiology, Malopolska Centre of Biotechnology, Jagiellonian University, Gronostajowa 7A, Krakow 30-387, Poland

ABSTRACT

Proliferating cell nuclear antigen (PCNA) is a multifunctional protein present in the nuclei of eukaryotic cells that plays an important role as a component of the DNA replication machinery, as well as DNA repair systems. PCNA was recently proposed as a potential non-oncogenic target for anti-cancer therapy. In this study, using the Systematic Evolution of Ligands by EXponential enrichment (SELEX) method, we developed a short DNA aptamer that binds human PCNA. In the presence of PCNA, the anti-PCNA aptamer inhibited the activity of human DNA polymerase δ and ε at nM concentrations. Moreover, PCNA protected the anti-PCNA aptamer against the exonucleolytic activity of these DNA polymerases. Investigation of the mechanism of anti-PCNA aptamer-dependent inhibition of DNA replication revealed that the aptamer did not block formation, but was a component of PCNA/DNA polymerase δ or ε complexes. Additionally, the anti-PCNA aptamer competed with the primer-template DNA for binding to the PCNA/DNA polymerase δ or ε complex. Based on the observations, a model of anti-PCNA aptamer/PCNA complex-dependent inhibition of DNA replication was proposed.

INTRODUCTION

Proliferating cell nuclear antigen (PCNA) is a key component of the DNA replication and DNA repair machineries in eukaryotes (1). Although PCNA was long considered a nuclear protein, recent studies indicate that it may also function in the cytoplasm, where it has been proposed to regulate neutrophil lifespan (2), and on the cell surface, where it acts as a ligand for the natural cytotoxicity receptor NKp44 to regulate the activation of natural killer cells (3). The PCNA monomer is composed of N- and C-terminal domains connected by an inter-domain connecting loop (IDCL). PCNA monomers spontaneously form a trimeric ring-like structure (4,5). During DNA replication, the PCNA trimer is loaded onto the DNA double helix by the Replication Factor C (RFC) complex, and slides bi-directionally along the DNA duplex (6). In recent decades, a large number of proteins involved in DNA replication, repair, cell cycle control, epigenetic regulation, cell survival and metabolism have been shown to interact with PCNA (7,8). PCNA not only functions as a docking platform for proteins involved in DNA metabolism, but it also stimulates the activity of some enzymes such as DNA polymerase (pol) δ, Fen1 and DNA ligase I (9,10). Analysis of the amino acid sequences of PCNA-interacting proteins led to the identification of the PCNA-Interacting Protein (PIP)-box motif, characterized by the consensus sequence Q-xx-(h)-x-x-(a)-(a), where h and a represent residues with moderately hydrophobic and aromatic side chains, respectively, while x is any residue (8,11). Other motifs have since been reported, including the KA-box (12) and the AlkB homolog 2 PCNA-interacting motif (APIM) identified in the sequence of human AlkB2 homolog 2, an oxidative demethylase involved in DNA damage repair (13). The affinity between PCNA and PCNA-interacting proteins can be controlled by post-translational modifiers (14).

The documented functions of PCNA in DNA replication and repair led to the proposal that PCNA may be a non-oncogenic target for anti-cancer therapy (15–17). It is anticipated that the application of molecules inhibiting binding between PCNA and PCNA-interacting proteins, in combination with other compounds directed at oncogenic targets, could increase the effectiveness of anti-cancer therapies. Previous attempts to block interactions between PCNA and PCNA-interacting proteins have focused on peptides and small molecules (18,19). However, the toxicity and im-

munogenicity of these molecules for human was not tested. Therefore, identifying alternative drug candidates targeting PCNA remains a priority. Among the molecules that could potentially fulfil such criteria are DNA aptamers, single-stranded deoxyoligonucleotides with the ability to adopt different secondary and tertiary structures. Aptamers can recognize a broad range of targets including low molecular weight molecules such as ions, vitamins and antibiotics, as well as high molecular weight molecules including enzymes and antibodies. DNA aptamers have been extensively studied as potential drug candidates and diagnostic tools. This is mainly due to their relatively inexpensive synthesis, low immunogenicity, high specificity and strong affinity for specific targets. Moreover, simple chemical modification of DNA aptamers can increase their specificity and stability [20,21]. For example, the DNA aptamer AS1411 was shown *in vitro* to effectively eliminate cancer cells over-expressing nucleolin on their surface [22]. Systematic Evolution of Ligands by EXponential enrichment (SELEX) is the classical DNA aptamer selection method first described in the early 1990s [23,24]. In SELEX, a target molecule is exposed to a synthetic ssDNA aptamer library composed of $10^{14}-10^{15}$ different oligonucleotides. The ssDNA fragments bound to the target are amplified using polymerase chain reaction (PCR), and the new pool of ssDNA for the next round of selection is prepared. After several rounds of selection, aptamers specific to target molecules are usually obtained. In the present study, we identified and characterized a PCNA-binding DNA aptamer capable of blocking DNA replication. The possible mechanism of anti-PCNA aptamer/PCNA complex-dependent DNA replication inhibition is discussed.

MATERIALS AND METHODS

Chemicals, plasmids and antibodies

All chemicals used for buffers and solutions were obtained from Sigma-Aldrich and Merck unless mentioned otherwise. Oligonucleotides were obtained from IBA GmbH (Germany). The template plasmid pDNR-LIB harboring human PCNA cDNA was purchased from ImaGenes GmbH (Germany). Primary anti-DNA pol δ p125 subunit goat polyclonal antibody (sc-8796), anti-DNA pol ε p261 subunit monoclonal antibody (CRL-2284) and anti-human PCNA monoclonal antibody (PC10) were purchased from Santa Cruz (USA), ATCC (UK) and Sigma-Aldrich (USA), respectively. Anti-human PCNA rabbit polyclonal antiserum was produced at Kyushu University. Goat anti-mouse IgG conjugated with HRP and goat anti-rabbit IgG conjugated with HRP secondary antibodies were purchased from Bio-Rad (USA), while rabbit anti-goat IgG conjugated with HRP was from Zymed Laboratories.

Cloning, protein production and purification

The open reading frame (ORF) encoding human PCNA was amplified using Phusion High-Fidelity DNA polymerase (Thermo Fisher Scientific, Lithuania). The PCR product amplified using primers HisPCNAF (5′-CAGGATCCGATGTTCGAGGCGCGCCTGGT CCAGGGCTC-3′) and HisPCNAR (5′-CCCAAGCTT CTAAGATCCTTCTTCATCCTCG-3′) was cloned into the pETDuet-1 vector (Novagen, Germany) using BamHI and HindIII restriction enzymes to create a vector encoding HisTag-PCNA. The PCR product amplified using primers StrepPCNAF (5′-CATATGGCTAGCTGGAGCCAC CCGCAGTTCGAAAAAGGCGCCATGTTCGAGGC GCGCCTGGTCCAGGGCTC-3′) and StrepPCNAR (5′-GCGGATCCCTAAGATCCTTCTTCATCCTCGA TCTTG-3′) was cloned into the pJET1.2 vector (Thermo Fisher Scientific), digested with NdeI and BamHI restriction enzymes and subcloned into the pET29a vector (Novagen) to create a plasmid encoding StrepTag-PCNA.

The *Escherichia coli* BL21 (DE3) CodonPlus-pRIL strain was used for protein production. Cells carrying plasmids harboring human PCNA were grown at 37°C using LB medium supplemented with 25 mg/l chloramphenicol and 50 mg/l kanamycin (pET29a) or 100 mg/l ampicillin (pETDuet-1). When the absorbance at 600 nm (OD_{600}) of the culture reached ∼0.6, protein overexpression was induced using 1 mM isopropyl β-D-1-thiogalactopyranoside (IPTG). Culturing was continued with vigorous shaking at 37°C for 4 h. Cells were harvested by centrifugation (5 min, 8000 × *g*, 4°C). HisTag-PCNA and StrepTag-PCNA bacteria were resuspended in binding buffer A (50 mM NaH_2PO_4, 300 mM NaCl, 10 mM imidazole, pH 8.0) and buffer B (100 mM TRIS–HCl pH 8.0, 150 mM NaCl, 1 mM ethylenediaminetetraacetic acid (EDTA)), respectively. Sonication was then performed for 8 min (5 s pulses and 10 s pauses) using an Omni-Ruptor 4000 sonicator (OMNI International Inc., USA). HisTag-PCNA and StrepTag-PCNA lysates were centrifuged (30 min, 30 000 × *g*, 4°C) and supernatants were loaded onto HisTrap FF Ni Sepharose (GE Healthcare, Sweden) and Strep-Tacin columns (IBA GmbH), respectively. Protein purification was performed according to the protocols supplied by the manufacturers. After elution from the nickel resin, HisTag-PCNA was dialyzed into buffer C (50 mM TRIS–HCl pH 7.6) and loaded onto an ion exchange High Q column (Bio-Rad, USA). The bound protein was eluted using a linear NaCl gradient from 0 to 0.8 M. The purified HisTag-PCNA and StrepTag-PCNA were dialyzed against buffer C supplemented with 150 mM NaCl, glycerol was added to a final concentration of 15% (v/v), and proteins were frozen in liquid nitrogen and stored at −80°C for further experiments. Tag-free human PCNA, and DNA pol δ and ε, were produced and purified as described previously [25–27].

SELEX procedure and aptamer cloning

Selection of DNA aptamers was performed using the SELEX method as described previously [28–30] with minor modifications. Trimeric StrepTag-PCNA was used as the selection target. The protein was covalently immobilized to cyanogen bromide-activated Sepharose 4B resin (Sigma-Aldrich, USA) according to the manufacturer's instructions. The DNA library employed was composed of molecules containing a 40-nucleotide random region and two 20-nt specific flanking fragments (5′-CATGCTTCCCCAGGGAGATG(N)$_{40}$GAGGAA CATGCGTCGCAAAC-3′). Sepharose beads with immobilized human StrepTag-PCNA were mixed with 1 μg

of ssDNA (except for the first selection cycle in which 25 μg of the synthetic DNA library was used) in buffer D (137 mM NaCl, 12.3 mM KCl, 10 mM Na_2HPO_4, 2 mM KH_2PO_4, 5 mM $MgCl_2$, 0.1% v/v Tween 20, pH 7.4) and incubated for 1 h at RT. Beads were then washed seven times using buffer D and used as a template for PCR in 50 μl reactions containing $1 \times$ PCR buffer (10 mM TRIS–HCl pH 8.8, 50 mM KCl, 0.08% v/v Nonidet P40, 2.5 mM $MgCl_2$), 500 μM dNTPs, 1 μM forward (5′-CATGCTTCCCCAGGGAGATG-3′) and reverse (5′-phosphate-GTTTGCGACGCATGTTCCTC-3′) primers, 1.5 units of Taq polymerase (Thermo Scientific) and the aptamer template. The reaction conditions were 94°C for 5 min, followed by 24 cycles of 94°C for 30 s, 55°C for 30 s and 72°C for 30 s, and a final amplification at 72°C for 5 min, performed in a gradient thermocycler. The PCR product was precipitated using isopropanol, and ssDNA for the next round of selection was prepared by digestion of the PCR product with exonuclease Lambda (Thermo Scientific, Lithuania) according to the protocol supplied by the producer. Finally, ssDNA was purified using a standard phenol/chloroform extraction procedure followed by isopropanol precipitation. The quality and concentration of ssDNA were evaluated by 8% DNA denaturing polyacrylamide gelelectrophoresis (PAGE). ssDNA molecules obtained after 12 rounds of SELEX were cloned into the pTZ57R/T vector using the InsTAclone PCR Cloning Kit (Thermo Fisher Scientific), and constructs were analyzed by DNA sequencing.

ELISA

Ni-coated microplates (Thermo Fisher Scientific) were incubated with 15 pmol of HisTag-protein (PCNA or GST, respectively) in 100 μl of Phosphate-buffered saline (PBS) o/n at 4°C. Next, wells were washed three times using PBS-T (PBS containing 0.05% v/v Tween-20) and blocked using PBS supplemented with 1% (w/v) BSA for 2 h at RT. After washing with PBS-T, biotinylated A1 (5′-CATGCTTCCCCAGGGAGATGCCTATGG TCCCCGCGTAGGTGGCAGCTCAAACCCGATTC GAGGAACATGCGTCGCAAAC-3′) or reference (Ref; 5′-(ACTG) × 19 ACT -3′) aptamer was added to the wells to a final concentration of 4 μM and plates were incubated for 1 h at RT with gentle agitation. After washing with PBS-T to remove unbound aptamers, horseradish peroxidase (HRP)-conjugated streptavidin (R&D Systems, USA) was added to the wells and incubated for 30 min at RT. Wells were washed again with PBS-T before the HRP chromogenic substrate (R&D Systems) was added. The reaction was stopped by addition of 1 M H_2SO_4, and the absorbance at 450 nm was measured using a microplate reader (Infinite-Pro Tecan 200, Tecan, Switzerland).

Pull-down assay

Pull-down assays were performed using a universal spin column (MoBiTec, Germany) and High Capacity Streptavidin Agarose (HCSA) Resin (Thermo Fisher Scientific). HCSA resin suspension was washed with distilled water and equilibrated with buffer AS (50 mM TRIS–HCl pH

7.5, 300 mM NaCl, 0.01% v/v Tween 20), and 20 μl of 50% (w/v) streptavidin-agarose resin was incubated with 800 pmol of the 5′-biotinylated aptamer in 300 μl of buffer AS for 1 h at RT with gentle agitation. Beads were washed three times with buffer AS (unless stated otherwise), incubated with 2 nmol of HisTag-PCNA protein or 5 mg of total protein extract in 500 μl of buffer AS for 1 h at 4°C, then washed four times with buffer AS. Aptamer-bound protein was denatured by incubation in GLB buffer (50 mM TRIS–HCl pH 6.8, 2% w/v sodium dodecyl sulphate (SDS), 2% w/v bromophenol blue, 10% v/v glycerol, 200 mM β-mercaptoethanol) at 95°C for 5 min. In the case of PCNA purification from *E. coli* total protein extract, protein was first eluted with buffer AE (50 mM TRIS–HCl pH 7.5, 500 mM NaCl, 300 mM guanidine hydrochloride, 0.01% v/v Tween 20), 2 × GLB buffer (50 mM TRIS–HCl pH 6.8, 2% w/v SDS, 0.1% w/v bromophenol blue, 10% v/v glycerol, 100 mM dithiothreitol (DTT)) was added and the sample was denatured at 95°C for 5 min. Samples were analyzed by 12% (v/v) SDS-PAGE followed by Coomassie brilliant blue staining.

α-PCNA aptamer impact on PCNA/DNA pol δ and PCNA/DNA pol ε interaction

DNA pol δ containing the HisTag-p50 subunit (0.8 pmol) was conjugated with Ni Sepharose High Performance beads (GE, Sweden), and 1.3 pmol of DNA pol ε was conjugated with anti-FLAG M2 affinity gel (Sigma-Aldrich, USA) in PDE buffer (25 mM HEPES-NaOH pH 7.8, 50 mM NaCl, 0.01% v/v NP40, 10% v/v glycerol). Beads were incubated with 4 pmol of PCNA and 5 pmol of α-PCNA or reference1 (Ref1; 5′-(ACTG) × 12 A-3′) aptamer in a 20 μl volume at 4°C for 30 min. Subsequently, beads were washed three times with PDE buffer (supplemented with 20 mM imidazole when DNA pol δ was used), suspended in 2 x GLB buffer and denatured at 95°C for 3 min. Next, protein samples were separated by 10% (v/v) SDS-PAGE followed by western blotting. DNA pol δ, DNA pol ε and PCNA were detected using anti-p125 and -p261 antibodies, and anti-human PCNA polyclonal serum, respectively.

Impact of α-PCNA aptamer on DNA pol δ and ε binding to 30/90-mer primer-template DNA

A 100 pmol sample of 30/90-mer DNA template generated by annealing 100 pmol of biotinylated 90-mer template (5′-TGAGGTTCAGCAAGGTGATGCTTTAGATTTT TCATTTGCTGCTGGCTCTCAGCGTGGCACTGT TGCAGGCGGTGTTAATACTGACCGCCT-biotin-3′) with 200 pmol of 30-mer primer (5′-CAGTGCCACGC TGAGAGCCAGCAGCAAATG-3′) was conjugated with 50 μl of Streptavidin Agarose Ultra Performance beads (Solulink, USA). A 1 pmol sample of 30/90-mer DNA template immobilized to streptavidin-agarose beads was incubated with 1 pmol of PCNA, 300 fmol of DNA pol δ and 500 fmol of the indicated aptamer, or 1 pmol of PCNA, 400 fmol of DNA pol ε and 250 fmol of the indicated aptamer, at 4°C for 10 min. Subsequently, beads were washed three times with PDE buffer, suspended in 2 x GLB buffer and denatured at 95°C for 3 min. Bound

proteins were separated by 10% (v/v) SDS-PAGE followed by western blotting. DNA pol δ and ε were detected using anti-p125 and -p261 antibodies, respectively.

Western blotting

Proteins were separated by 12% (v/v) SDS-PAGE and transferred onto a PVDF membrane (Millipore, USA). Membrane was washed three times with PBS-T, blocked with 5% (w/v) milk in PBS-T (PBS-TM) and incubated with primary antibody (1:10 000 dilution) or undiluted serum o/n at 4°C. After washing three times with PBS-TM, the membrane was incubated with the appropriate secondary antibody (1:10 000 dilution) for 1 h at RT. After several washes, protein detection was performed using Clarity Western ECL Blotting Substrate (Bio-Rad) and the BioSpectrum Imaging System (UVP Ultra-Violet Products Ltd, UK).

Computational analysis

Modeling of α-PCNA aptamer secondary structure and theoretical prediction of the ΔG parameter were performed using the Mfold server (31). Calculations were performed at 25°C with 300 mM NaCl.

K_D determination by pull-down assay

A volume of 40 μl of HCSA resin suspension (in excess to bind all biotinylated aptamer molecules in each sample) was washed with distilled water and equilibrated with buffer D (137 mM NaCl, 12.3 mM KCl, 10 mM Na_2HPO_4, 2 mM KH_2PO_4, 5 mM $MgCl_2$, 0.1% v/v Tween 20, pH 7.4). Beads were incubated in 60 μl of buffer D with 5′-biotinylated α-PCNA aptamer (concentration range from 0 to 100 μM) for 1 h at RT with gentle agitation. Subsequently, the complete immobilization of α-PCNA aptamer to HCSA resin was confirmed by measuring the absorbance at 260 nm. Next, beads were washed five times with buffer D and incubated with 100 nM HisTag-PCNA for 1 h at RT. After incubation, beads were centrifuged, 2 × GLB buffer was added to the supernatant, and samples were incubated at 95°C for 5 min and separated by 12% (v/v) SDS-PAGE followed by Coomassie brilliant blue staining. Densitometric analysis of the gel was performed using a Multispectral Imaging System IMAGER with Launch VisionWorksLS (version 6.8) software. The dissociation constant (K_D) calculation was performed using GraphPad Prism software (La Jolla, CA, USA). Using the equilibrium concentration of HisTag-PCNA/α-PCNA aptamer as a function of free α-PCNA aptamer (total aptamer), the K_D of the tested complex was calculated.

Calorimetric analysis of K_D and binding stoichiometry

All isothermal titration calorimetry (ITC) experiments were carried out at 25°C using a VP-ITC instrument (MicroCal, USA). HisTag-PCNA and α-PCNA aptamer solutions were dialyzed overnight against buffer D. All solutions were degassed under vacuum prior to use in ITC experiments. Typically, 25 injections of 650−703 μM α-PCNA aptamer solution (ligand) were applied to the calorimeter cell (1.4355 ml

volume) filled with buffer D and 30−32 μM HisTag-PCNA (calculated as a monomer concentration). The first injection was 3 μl, and subsequent injections were 3, 8 or 10 μl. The injection speed was 0.5 μl/s with 4 min intervals between injections. To ensure proper mixing after each injection, a constant stirring speed of 300 rpm was maintained throughout the experiment. The α-PCNA aptamer dilution (reference) experiments were analyzed according to the dimer dissociation model provided in Origin software (version 7.0, OriginLab, Northampton, MA, USA). In the case of complex formation experiments, a double correction was used prior to data analysis. First, the heat of the α-PCNA aptamer dilution was subtracted, and the mean value of the heat after saturation was then subtracted. Data were analyzed according to the one set of sites model provided in Origin 7.0 software.

Circular dichroism (CD) spectroscopy analysis

All circular dichroism (CD) spectroscopy measurements were recorded on a JASCO J-710 (JASCO Co., Japan) spectropolarimeter equipped with a circulating water bath (JULABO Labortechnik GmbH, Germany). Buffer D was used for all experiments. Spectra were recorded in the range of 190−320 nm for the α-PCNA aptamer, 190−250 nm for HisTag-PCNA and 240−320 nm for the α-PCNA aptamer/HisTag-PCNA complex, with 1 nm resolution. The appropriate path length and sample concentration were chosen for every measurement to maintain the photomultiplier voltage below 700 V. Three scanning acquisitions were accumulated and averaged to yield the final spectrum. CD spectra were corrected for the buffer baseline. The ellipticity was recalculated to give the difference in extinction coefficients ($\Delta\varepsilon$) when possible. Spectra were normalized to path length, peptide bond concentration for proteins and nucleotide concentration for ssDNA. Temperature-dependent measurements were performed using a 1 mm path length, and a 17 or 34 μM α-PCNA aptamer concentration. The signal at 270 nm was recorded over the range of 20−80°C. The heating or cooling rate was 1.0°C per min. Raw temperature scans were processed using Origin software (version 9.1.0) according to a simple model of two-state denaturation assuming both $\Delta H°$ and ΔS are constant (i.e. $\Delta C_P = 0$ for the melting transition).

DNA pol assay with oligo dT/poly dA primer-template DNA

DNA synthesis was performed in 5 μl reactions containing buffer E (30 mM HEPES-NaOH pH 7.8, 7 mM $MgCl_2$, 0.01% w/v BSA, 500 μM DTT) supplemented with 50 μM TTP, [α-^{32}P] TTP (Perkin Elmer, USA), 800 fmol of oligo(dT)/poly(dA) (dT/dA) primer-template DNA (200 pmol as polynucleotide), 50 fmol of DNA pol δ or ε, 1 pmol of PCNA and the indicated amount of tested aptamer at 37°C for 15 min. Each reaction mixture was adsorbed to DE81 paper (Whatman, UK) and washed four times for 3 min each time with 0.5 M Na_2HPO_4. ^{32}P-TMP incorporated into dT/dA was measured by Cherenkov counting with a liquid scintillation counter (Beckman, USA).

DNA pol assay with 28/90-mer primer-template DNA

A 10 pmol sample of 28-mer primer (5′-AGGCGGT CAGTATTAACACCGCCTGCAA-3′) was labeled with [γ-^{32}P] ATP (Perkin Elmer) using T4 polynu-cleotide kinase (Clontech, USA) at 37°C for 1 h and purified by phenol-chloroform extraction and ethanol precipitation. The labeled 28-mer primer was mixed with a 1.5-fold molar excess of 90-mer template (5′-TGAGGTTCAGCAAGGTGATGCTTTAGATTTT TCATTTGCTGCTGGCTCTCAGCGTGGCACTGTT GCAGGCGGTGTTAATACTGACCGCCT-3′). The primer extension reaction was performed in a 5 μl reaction containing buffer E supplemented with 50 μM dNTP, 800 fmol of labeled 28/90-mer primer-template DNA, 50 fmol of DNA pol δ or ε, 1 pmol of PCNA and the indicated amount of tested aptamer at 37°C for 15 min. Next, formamide dye (98% v/v deionized formamide, 10 mM EDTA, 0.025% w/v xylene cyanol, 0.025% w/v bromophenol blue) was added and samples were incubated at 95°C for 3 min. Denatured samples were separated on a 10% (v/v) polyacrylamide gel containing 7 M urea in TBE buffer (100 mM TRIS–HCl pH 8.0, 100 mM boric acid, 2 mM EDTA). The gel was fixed with a mixture of 15% (v/v) methanol and 15% (v/v) acetic acid for 5 min, followed by washing with water for 5 min. Products resulting from the 28-mer extension were detected by autoradiography with a FLA-7000 phosphorimager (GE Healthcare, USA).

DNA pol assay with Ref1 or α-PCNA aptamer as primer-template DNA

A 10 pmol sample of aptamer was labeled with [γ-^{32}P] ATP (Perkin Elmer) using T4 polynucleotide kinase at 37°C for 1 h and purified by phenol-chloroform extraction followed by ethanol precipitation. Primer extension was performed in a 5 μl reaction mixture containing buffer E supplemented with 50 μM dNTP, 160 fmol of labeled Ref1 or α-PCNA aptamer, 80 fmol of DNA pol δ or ε and 1 pmol of PCNA at 37°C for 15 min. Samples were then treated as described above in the DNA pol assay with a 28/90-mer primer-template DNA.

Electrophoretic mobility shift assay (EMSA)

A 10 pmol sample of the tested aptamer was labeled with [γ-^{32}P] ATP using T4 polynucleotide kinase, and 10 fmol of the tested aptamer was incubated in a 5 μl reaction mixture containing buffer E supplemented with 20 mM NaCl, 50 or 100 fmol of DNA pol δ or ε, 1 pmol of PCNA, and 0, 0.5 or 1 pmol of 28/90-mer primer-template DNA at 32°C or on ice for 10 min. Aptamer/protein complexes were fixed for 5 min by addition of 0.5 μl of 10% (v/v) glutaraldehyde at 32°C. The crosslinking reaction was terminated by addition of 0.5 μl of electrophoretic mobility shift assay (EMSA) loading buffer (100 mM TRIS-HCl pH 8.0, 20% w/v sucrose, 0.1% w/v bromophenol blue). Next, samples were separated on a 5% (v/v) polyacrylamide gel in TAE buffer (40 mM TRIS–HCl pH 8.0, 20 mM acetate, 1 mM EDTA). The gel was fixed in a mixture containing 15% (v/v) methanol and 15% (v/v) acetic acid for 5 min, followed by washing with water

for 5 min. The labeled aptamer was detected by autoradiography with a FLA-7000 phosphorimager (GE Healthcare).

Statistical analysis

The significance of the effects of the presence of PCNA (two levels: PCNA present or absent) and the type of aptamer (three levels: Ref1 aptamer, α-PCNA aptamer or no aptamer) on DNA pol activity was assessed using two-way ANOVA. When a significant effect of the type of aptamer was detected with ANOVA, Tukey's test was used to assess differences in the means between particular types of aptamers. Measured values were log-transformed before analysis. Calculations were performed using R software. To estimate the relative inhibitory concentration of aptamers (half-maximal inhibitory concentration; IC50) on DNA pol activity, the 4-parameter logistic model was fitted to the results of DNA pol assays using Mathematica 9.0 (Wolfram Research, USA).
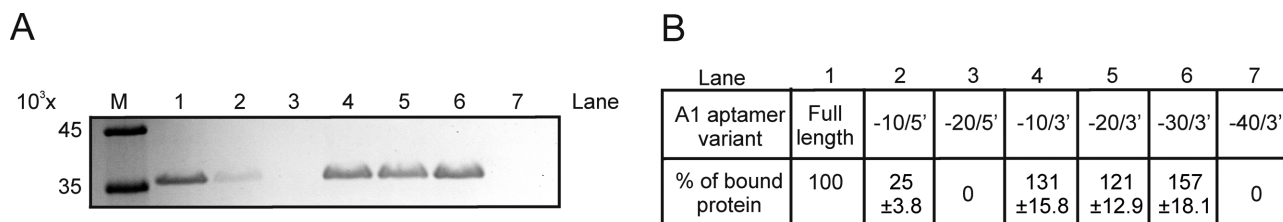
RESULTS

### Selection of anti-PCNA aptamers

The SELEX method was employed to generate a DNA aptamer able to bind tightly to human PCNA. After 12 rounds of selection against StrepTag-PCNA, selected aptamers were cloned and sequenced, and aptamer A1 (5′-CATGCTTCCCCAGGGAGATGCCTATGGTCCC CGCGTAGGTGGCAGCTCAAACCCGATTCGAGG AACATGCGTCGCAAAC-3′) was identified. The pull-down assay was employed to verify the binding of A1 to human PCNA, and unlike the Ref aptamer, A1 was able to pull-down HisTag-PCNA from solution (Supplementary Figure S1A). The binding of aptamer A1 to PCNA was also subsequently confirmed using ELISA (Supplementary Figure S1B).

Determination of the region of aptamer A1 required for PCNA binding

To determine the region of aptamer A1 essential for efficient binding to human PCNA, full-length A1 and variants shortened at the 5′ or 3′ end (Table 1) were tested in pull-down assays (Figure 1A). The −10/5′ variant bound only ~25% of the amount of PCNA bound by the full-length A1 aptamer (Figure 1B). Binding was not detected between PCNA and the −20/5′ variant. Interestingly, the A1 aptamer variant with 30 nt removed from the 3′ end (−30/3′) bound ~160% PCNA and was therefore ~60% more efficient than the full-length A1 aptamer. However, further removal of nucleotides from the 3′ end (−40/3′ A1 aptamer variant) led to a complete loss of affinity for PCNA. Thus, the 49-nt A1 aptamer variant shortened only by 30 nt from the 3′ end (5′-CATGCTTCCCCAGGGAGATGCCTAT GGTCCCCGCGTAGGTGGCAGCTCA-3′ ssDNA) was used for subsequent experiments and is referred to henceforth as the α-PCNA aptamer. To verify the binding between the α-PCNA aptamer and tag-free PCNA, the protein was overexpressed in *E. coli*. HCSA resin with immobilized 5′-biotinylated aptamer was incubated with *E. coli* total protein extract containing PCNA, unbound proteins

A

B

Lane		1	2	3	4	5	6	7
A1 aptamer variant	Full length	-10/5'	-20/5'	-10/3'	-20/3'	-30/3'	-40/3'
% of bound protein	100	25 ±3.8	0	131 ±15.8	121 ±12.9	157 ±18.1	0

Figure 1. Identification of the A1 aptamer region necessary for PCNA binding. (**A**) Pull-down analysis of the binding of A1 aptamer variants shortened at the 5′ or 3′ end to PCNA. Aptamers were bound to streptavidin-agarose resin and incubated with HisTag-PCNA. After washing unbound proteins, bound HisTag-PCNA was denatured, separated by 12% SDS-PAGE and stained with Coomassie brilliant blue. Lane M, protein mass marker; 1, full-length A1; 2, −10/5′ variant; 3, −20/5′ variant; 4, −10/3′ variant; 5, −20/3′ variant; 6, −30/3′ variant (referred to as the α-PCNA aptamer); 7, −40/3′ variant. The presented results are representative. (**B**) Densitometric analysis of HisTag-PCNA bound to A1 aptamer variants presented on panel (A). The results are normalized relative to the signal from the protein sample bound to the full-length aptamer (100%). Results are means of triplicate measurements, and errors represent standard deviation.
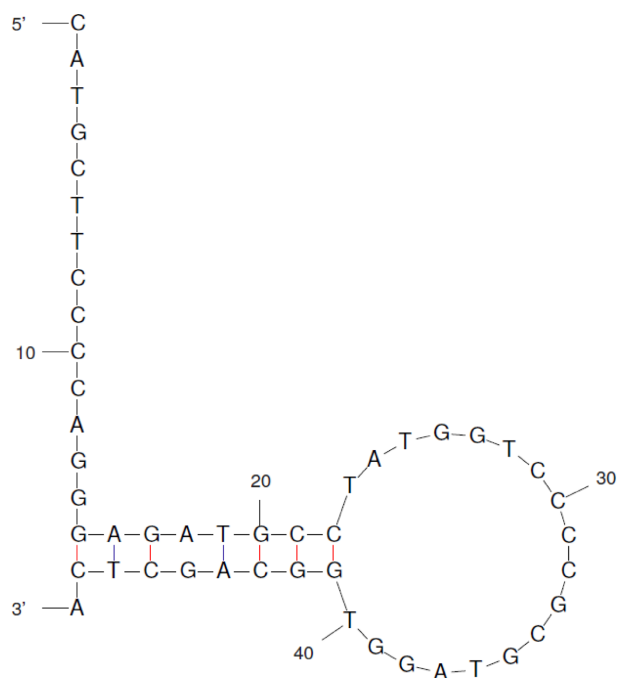
Figure 2. Representative putative secondary structure of the α-PCNA aptamer predicted by the Mfold server. The aptamer structure was modeled using the Mfold web server at 25°C and 300 mM NaCl.

Figure 3. Determination of the α-PCNA aptamer/PCNA complex dissociation constant by pull-down assay. Biotinylated α-PCNA aptamer (concentration range from 0 to 100 μM) bound to streptavidin-agarose resin was incubated with 100 nM HisTag-PCNA. Unbound protein was denatured, separated by 12% SDS-PAGE and stained with Coomassie brilliant blue. Densitometric analysis of data from pull-down assays was performed using a Multispectral Imaging System IMAGER with Launch VisionWorksLS. The dissociation constant ($K_D = 5.1 \pm 0.59$ μM) of the complex was calculated based on the equilibrium concentration of HisTag-PCNA/α-PCNA aptamer as a function of free α-PCNA aptamer (total aptamer) using GraphPad Prism software. Results are the mean of triplicate measurements, and error bars represent standard deviation.

were removed by washing and bound protein was eluted. Unlike the Ref1 aptamer (data not shown), the α-PCNA aptamer bound to and successfully purified PCNA from the mixture of bacterial proteins (Supplementary Figure S2A and B).

Modeling the α-PCNA aptamer secondary structure

To predict the putative secondary structure of the α-PCNA aptamer, computational analysis was employed using the Mfold server. At 300 mM Na$^+$ concentration and 25°C, the aptamer was predicted to potentially adopt two similar secondary structures, and the structure shown in Figure 2 with a calculated free energy (ΔG) of −6.62 kcal/mol is representative.

Characterization of the α-PCNA aptamer/PCNA complex

Determination of the K_D. To evaluate the affinity of the α-PCNA aptamer for PCNA, two different approaches were employed. The first was based on a pull-down assay in which a constant amount of HisTag-PCNA was titrated with increasing concentrations of α-PCNA aptamer (Figure 3). Densitometric analysis of the resulting gel was used to calculate the K_D of the α-PCNA aptamer/PCNA complex from the Hill slope of a one site-specific binding model. ITC was the second method used to characterize the α-PCNA aptamer/PCNA interaction. Similarly to the pull-down assay, HisTag-PCNA was titrated with increasing concentrations of α-PCNA aptamer. Exemplary raw isotherms of the reference measurement and the α-PCNA aptamer/PCNA-binding reaction are presented in Figure 4A. Both processes yielded similar endothermic deflections, but the heat of dilution of the α-PCNA aptamer (reference) had a higher am-

Table 1. A1 aptamer variants used in pull-down assays

A1 aptamer variant name	A1 aptamer variant sequence
Full length	5′-CATGCTTCCCCAGGGAGATGCCTATGGTCCCCGCGTAGGTGGCAGCTCAAACCCGATTCGAGGAACATGCGTCGCAAAC-3′
−10/5′	5′-CAGGGAGATGCCTATGGTCCCCGCGTAGGTGGCAGCTCAAACCCGATTCGAGGAACATGCGTCGCAAAC-3′
−20/5′	5′-CCTATGGTCCCCGCGTAGGTGGCAGCTCAAACCCGATTCGAGGAACATGCGTCGCAAAC-3′
−10/3′	5′-CATGCTTCCCCAGGGAGATGCCTATGGTCCCCGCGTAGGTGGCAGCTCAAACCCGATTCGAGGAACATG-3′
−20/3′	5′-CATGCTTCCCCAGGGAGATGCCTATGGTCCCCGCGTAGGTGGCAGCTCAAACCCGATTC-3′
−30/3′	5′-CATGCTTCCCCAGGGAGATGCCTATGGTCCCCGCGTAGGTGGCAGCTCA-3′
−40/3′	5′-CATGCTTCCCCAGGGAGATGCCTATGGTCCCCGCGTAGG-3′
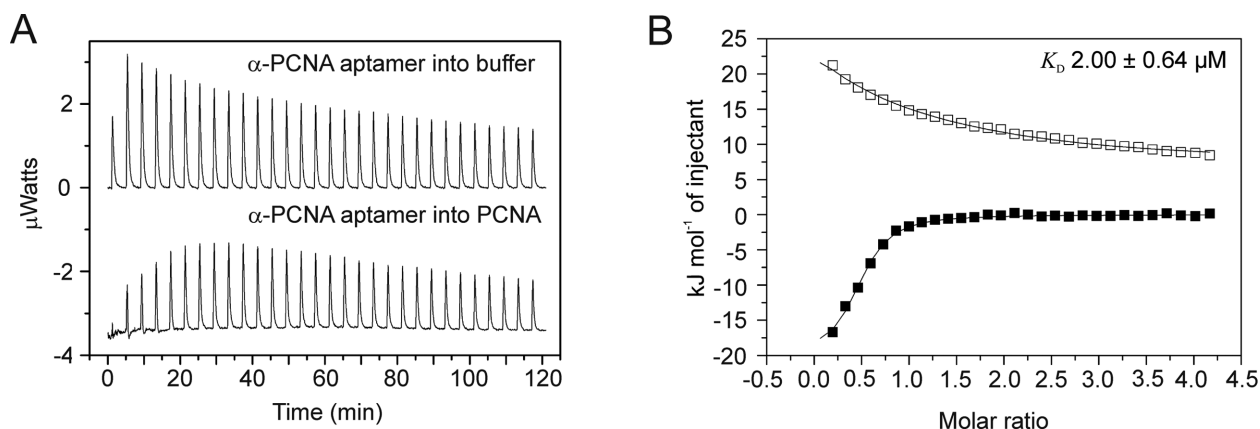
Figure 4. Determination of the α-PCNA aptamer/PCNA complex dissociation constant by ITC. (**A**) Raw calorimetric trace for α-PCNA dissociation and its titration into PCNA. (**B**) Integrated heats per mole of α-PCNA injected into buffer (open squares, reference measurement) and α-PCNA injected into PCNA solution after subtraction of reference measurements (solid squares). Solid lines represent the best fit of the dimer dissociation model (open squares) and the one set of sites model (solid squares) to experimental data. The calculated K_D value is 2.00 ± 0.64 μM.

plitude and decreased monotonically, unlike the titration of α-PCNA aptamer into HisTag-PCNA, which was accompanied by an initial increase followed by a distinct decrease. The large heat deflections accompanying α-PCNA aptamer dilution indicate a change in oligomeric state at high concentration (Figure 4A). For reference data, application of a simple dimer dissociation model provided a good fit, and global analysis of data from three independent experiments showed that the K_D for reference measurements was 0.51 ± 0.08 mM, and the $\Delta H°$ value was 52.7 ± 4.9 kJ/mol. The failure to achieve a perfect fit between this model and the obtained data may indicate a more complex mechanism of dissociation, such as the presence of higher order oligomers (data not shown). However, we assume that the monomeric form of α-PCNA dominates at low concentrations. The occurrence of dissociation during α-PCNA aptamer dilution suggests that reference measurements were not entirely correct, but the relatively high K_D value implies that this effect could be ignored. Subtraction of reference data from α-PCNA aptamer/PCNA data resulted in an exothermic sigmoidal signal, although the heat deflections did not decrease to zero by the end of the titration. The constant heat deflection accompanying the final few injections indicates a slight buffer mismatch resulting from incomplete dialysis of the protein. Based on this interpretation, the mean value of final five injections was treated as the offset value and subtracted from all data prior to further analysis. The final isotherm is shown in Figure 4B (solid squares). Binding of the α-PCNA aptamer to PCNA was correctly described by the one set of sites model. The calculated mean values of thermodynamic parameters, summarized in Table 2,

**Table 2.** Thermodynamic parameters of the α-PCNA aptamer/PCNA complex based on ITC analysis

N	0.48	± 0.11
K_A (M^{-1})	499 000	± 160 000
K_D (μM)	2.00	± 0.64
$\Delta H°$ (kJ/mol)	−20.63	± 1.38
$\Delta S°$ (J/mol K)	39.54	± 2.15
$\Delta G°$ (kJ/mol)	−32.5	± 0.8

N = stoichiometry; K_A and K_D = association and dissociation constants, respectively; ΔH, ΔS and ΔG = enthalpy, entropy and Gibbs free energy changes, respectively.

showed that the formation of the α-PCNA aptamer/PCNA complex was driven by both enthalpy and entropy. The obtained stoichiometry of 0.48 suggests that one PCNA trimer binds to 1.44 α-PCNA molecules.
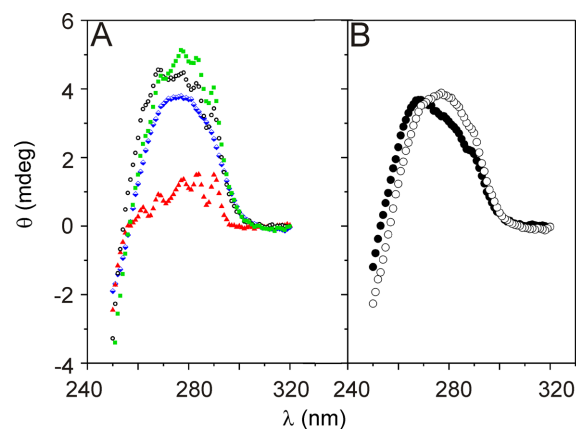
CD spectroscopy analysis of the α-PCNA aptamer

CD spectroscopy was employed to analyze the secondary structure of the α-PCNA aptamer. The position and low relative intensity of the positive long wavelength band at ∼270 nm and the negative band at ∼245 nm suggests that the α-PCNA aptamer partially adopts a typical B-form conformation (Figure 5A). Thermal denaturation of the α-PCNA aptamer was monitored to investigate its stability. The peak at 270 nm represents the maximum change in the CD spectrum; hence it was chosen to monitor aptamer unfolding. Sequential spectra were collected between 20 and 80°C in both increasing and decreasing directions, which confirmed the fully reversible nature of α-PCNA aptamer denaturation (Figure 5B). The presence of isodichroic points at 231.5 and 256.5 nm (Figure 5A, inset) implies a simple two-state mechanism for aptamer structural changes. Global analysis
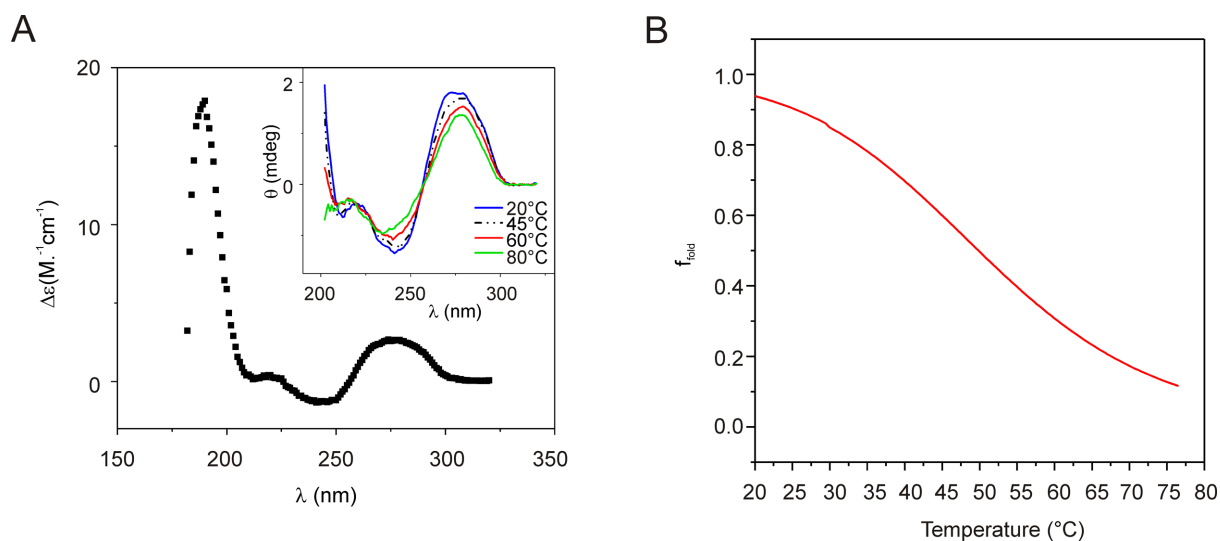
Figure 5. CD spectroscopic characterization of the α-PCNA aptamer as a function of temperature. (**A**) CD spectrum of the α-PCNA aptamer measured at 20°C. Inset shows CD spectra of the α-PCNA aptamer measured at 20°C (blue line), 45°C (black dotted line), 60°C (red line) and 80°C (green line). (**B**) Averaged thermal denaturation profile of the α-PCNA aptamer measured at 270 nm, based on three increases and two decreases of temperature. The folded fraction (f_{fold}) of the α-PCNA aptamer was calculated according to the estimated values of fully folded and unfolded forms. The line (red) is calculated based on the self-complementary strand melting model with $T_m = 51.4°C$ and $\Delta H° = -68.6$ kJ/mol.

of all recorded traces was performed based on the melting of self-complementary strand model with shared values of T_m and $\Delta H°$, and without thermal dependence of the ellipticity for folded and unfolded forms of the α-PCNA aptamer. This model provided a very good fit for the data and gave the following parameters: $T_m = 51.4 \pm 0.2°C$, $\Delta H° = -68.6 \pm 1.0$ kJ/mol, $\Delta S° = -211 \pm 3$ J/mol K and $\Delta G°_{25°C} = -5.9 \pm 0.1$ kJ/mol. The obtained parameters show that 91% of α-PCNA aptamer molecules were folded at 25°C, and 77% were folded at 37°C.

To test whether the binding of the α-PCNA aptamer to the target protein changes the structure of the aptamer, CD spectra analysis was limited to 250−320 nm, where the protein signal is typically significantly lower than the nucleic acid signal. Additionally, a >11-fold excess of protein was used to maximize DNA complexation. This CD analysis revealed evident differences between the summed spectra of independently measured α-PCNA aptamer and HisTag-PCNA, and spectra of the complex (Figure 6A). Spectral decomposition was performed according to calorimetric data, which revealed that the bound fractions of α-PCNA aptamer and HisTag-PCNA under these experimental conditions were 0.96 and 0.18, respectively. Using data from a sample composed of α-PCNA aptamer and HisTag-PCNA, the spectrum of the complex was calculated according to the following formula: (total spectrum recorded for complex mixture) − (0.04 × spectrum recorded for α-PCNA aptamer + 0.82 × spectrum recorded for HisTag-PCNA). To obtain a spectrum in which presumably no structural changes in substrates took place during complex formation, a simple sum of α-PCNA aptamer and HisTag-PCNA spectra measured separately based on their participation in the complex was calculated using the following formula: (0.96 × α-PCNA aptamer + 0.18 × HisTag-PCNA). The observed difference between both spectra was significant and associated with a shift in the wavelength maximum from 278 to 270 nm


Figure 6. Near-UV CD spectroscopy analysis of α-PCNA aptamer and PCNA association. Association of α-PCNA aptamer with PCNA was analyzed by CD. (**A**) Spectra of the α-PCNA aptamer (blue half-diamonds), HisTag-PCNA (red triangles) and α-PCNA aptamer/HisTag-PCNA (ratio, 1:11; open circles), and the calculated sum of separately measured α-PCNA aptamer and HisTag-PCNA spectra (green squares). (**B**) Spectra of the α-PCNA aptamer/PCNA complex without (open circles) and with (black solid circles) structural changes assumed.

(Figure 6B). This indicates changes in the secondary and/or tertiary structure of the participants as a result of complex formation. Hypsochromic shift rather cannot be attributed to the transition of PCNA aromatic amino acids because it would reflect changes of PCNA structure. Given stability and ordered structure of PCNA, under the experimental conditions employed, changes in the α-PCNA aptamer structure likely caused the observed differences.

Effect of the α-PCNA aptamer on DNA replication

To elucidate the impact of the α-PCNA aptamer on DNA replication, a set of *in vitro* assays was performed. First,
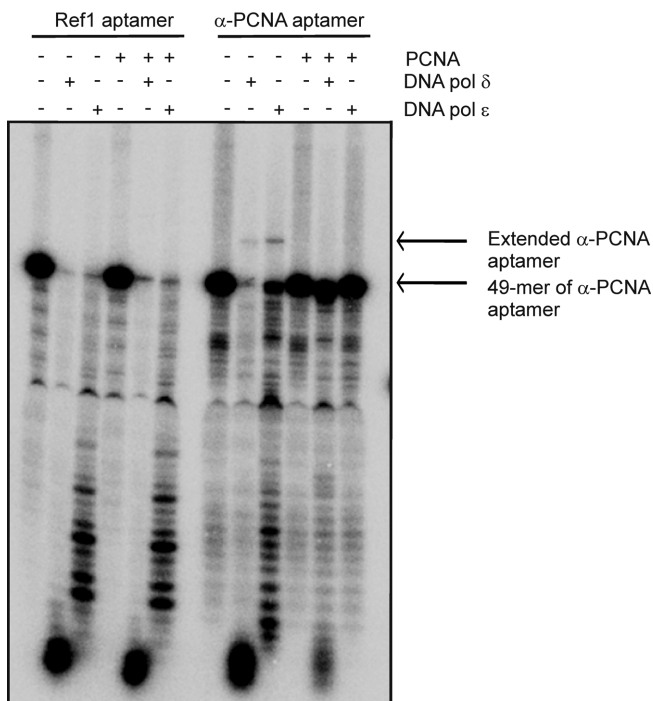
Figure 7. Evaluation of the α-PCNA aptamer as a potential primer-template DNA for DNA pol δ and ε. Extension of 160 fmol of 5′ ³²P-labeled Ref1 and the α-PCNA aptamer by DNA pol δ or ε was tested in the presence or absence of PCNA. Only the α-PCNA aptamer, in the absence of PCNA, was used as a primer-template DNA by both DNA pol δ and ε. Exonuclease degradation of 160 fmol of α-PCNA or Ref1 aptamer by DNA pol δ or ε was observed in the absence of PCNA. In the presence of PCNA and DNA pol δ or ε, degradation of Ref1 but not α-PCNA aptamer was detected. Samples were separated by 10% polyacrylamide gel containing 7 M urea. The signal was detected by autoradiography. Presented results are representative.

binding of the α-PCNA aptamer to HisTag-PCNA was assessed at 25 and 37°C, and interaction between PCNA and the α-PCNA aptamer was observed at both temperatures (Supplementary Figure S3). Based on the modeled putative secondary structure of the α-PCNA aptamer (Figure 2), we next tested whether it could serve as a primer-template DNA for DNA pol δ or ε. In the absence of PCNA, the α-PCNA aptamer was used by both DNA pol enzymes as a primer-template DNA, albeit with very low efficiency, but the reference (Ref1) aptamer was not used (Figure 7). By contrast, in the presence of PCNA, neither DNA pol δ nor ε was able to use the α-PCNA or Ref1 aptamer as a primer-template DNA. In the same experiment, the ability of the α-PCNA aptamer to function as a substrate for the exonucleolytic activity of DNA pol δ or ε was verified. We found that, in the absence of PCNA, both α-PCNA and Ref1 aptamers were degraded. However, when PCNA was present in the reaction mixture, the α-PCNA but not the Ref1 aptamer was protected against the exonucleolytic activity of DNA pol δ and ε.

Subsequently, the impact of the α-PCNA aptamer on the activity of human DNA pol δ (using a dT/dA primer-template DNA) was tested in the presence or absence of PCNA. This experiment clearly showed no significant impact of either the α-PCNA or Ref1 aptamer on DNA pol

δ activity in the absence of PCNA (Figure 8A). However, unlike the Ref1 aptamer, the α-PCNA aptamer inhibited the activity of DNA pol δ in the presence of PCNA (Figure 8A). Moreover, in the presence of PCNA and the α-PCNA aptamer, the activity of DNA pol δ was ∼3-fold lower than in the absence of PCNA and the presence of the α-PCNA aptamer. To evaluate the efficiency of DNA pol δ inhibition, the IC50 of the α-PCNA aptamer was determined (Figure 8B) and found to be in the nM range. In the next experiment, the impact of the α-PCNA aptamer on the activity of DNA pol δ was tested using a 28/90-mer primer-template DNA (Figure 8C). At a concentration of 300 nM α-PCNA aptamer, the activity of DNA pol δ was undetectable. As in the previous experiment (using a dT/dA primer-template DNA), the IC50 value of the α-PCNA aptamer was also in the nM range when the 28/90-mer primer-template DNA was used (Figure 8D). Additionally, a detailed analysis of 28-mer DNA extension (Figure 8C) in the absence of PCNA revealed the production of intermediate DNA replication products by DNA pol δ (Figure 8C, lane 11; PCNA-independent activity of DNA pol δ). Moreover, in the absence of PCNA and the presence of the α-PCNA aptamer, PCNA-independent DNA pol δ activity was not inhibited (Figure 8C, lane 12). However, in the presence of PCNA, the α-PCNA aptamer inhibited both the PCNA-dependent and PCNA-independent activity of DNA pol δ.

Next, the impact of the α-PCNA aptamer on DNA pol ε activity was analyzed. In the absence of PCNA, when a dT/dA primer-template DNA was used, a similar level of DNA pol ε inhibition was observed in the presence of both the α-PCNA and Ref1 aptamers (Figure 9A). Thus, this inhibition was probably due to the presence of an excess of oligonucleotides. However, in the presence of PCNA, a statistically significant difference between the α-PCNA and Ref1 aptamer, in the context of DNA pol ε activity inhibition, was clearly visible. Moreover, the difference in DNA pol ε activity in the presence of either only the α-PCNA aptamer, or both PCNA and the α-PCNA aptamer, was also statistically significant. Testing the impact of the α-PCNA aptamer on the activity of DNA pol ε using a 28/90-mer primer-template DNA yielded similar results to those obtained for the dT/dA primer-template DNA (Figure 9A, C and D). In both cases, the IC50 value of the aptamer was in the nM range.

Influence of the α-PCNA aptamer and PCNA on α-PCNA aptamer/PCNA/DNA pol complex formation

Analysis of the data from our studies indicated that the mechanism underlying the inhibition of DNA pol enzymes was not simply due to interference with the DNA pol/PCNA interaction. Therefore, we next tested whether the α-PCNA aptamer, PCNA and DNA pol δ or ε could form ternary complexes. Appropriate mixtures composed of DNA aptamer, PCNA and/or DNA pol were prepared, incubated at 4°C, fixed with glutaraldehyde and assessed by EMSA. The results demonstrated that binding between PCNA and DNA pol δ or ε was not abolished in the presence of the α-PCNA aptamer, and the aptamer was present in the complex with PCNA (Supplementary Figure S4) as well as the complex with DNA pol δ or ε, although only
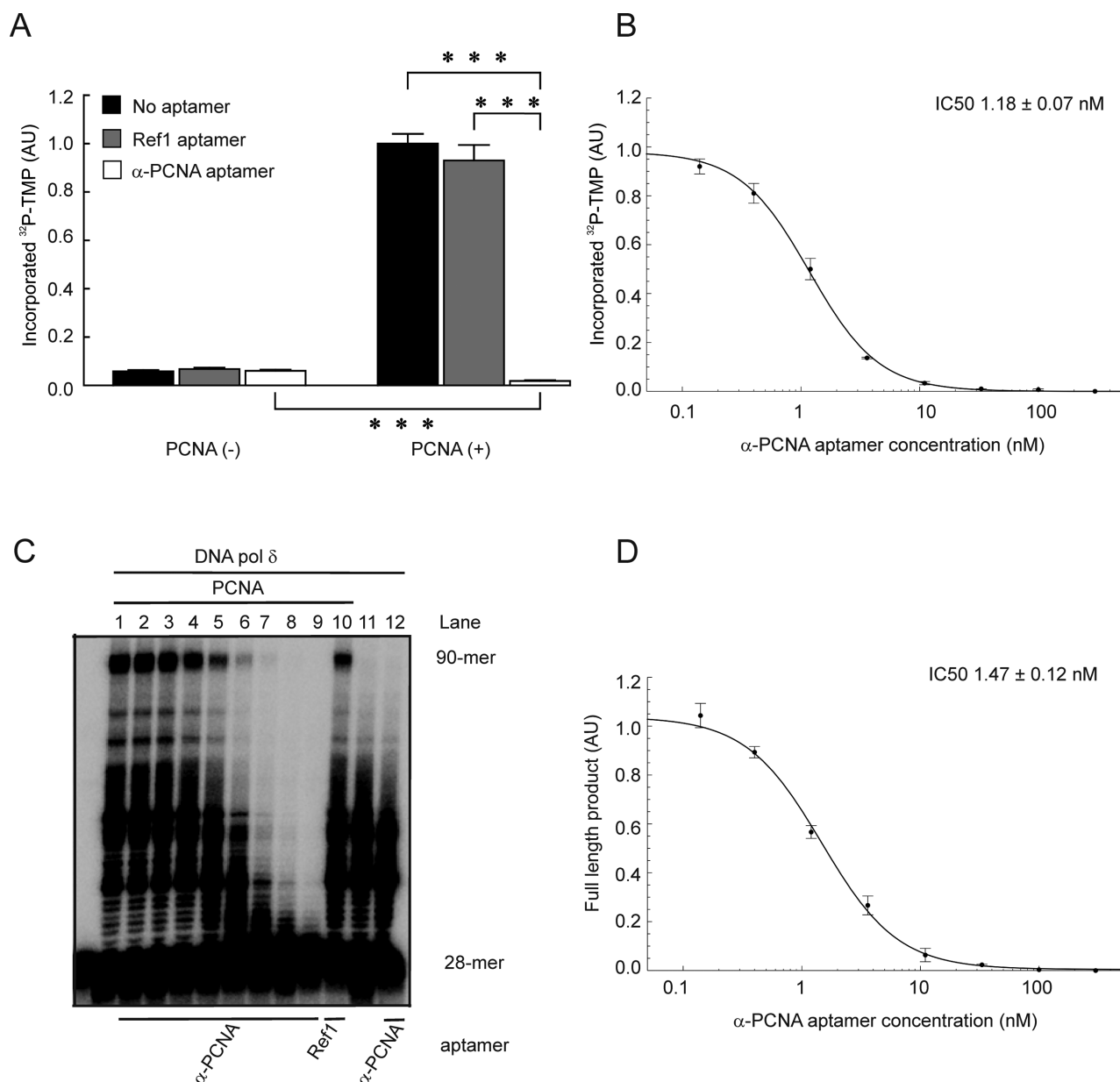
Figure 8. The impact of the α-PCNA aptamer on DNA pol δ activity in the presence or absence of PCNA. (**A**) Incorporation of ^{32}P-TMP into a dT/dA primer-template DNA by DNA pol δ in the presence or absence of PCNA and 100 nM α-PCNA or reference1 (Ref1) aptamer. The relative amount of ^{32}P-TMP incorporation was normalized against the mean amount of ^{32}P-TMP incorporated in the presence of PCNA and absence of aptamer. (**B**) Incorporation of ^{32}P-TMP into a dT/dA primer-template DNA by DNA pol δ in the presence of PCNA and increasing concentrations of α-PCNA aptamer (0.14, 0.4, 1.2, 3.6, 11.0, 33.0, 100 and 300 nM). Values are normalized against the amount of ^{32}P-TMP incorporated in the absence of the α-PCNA aptamer. (**C**) Extension of a 5′ ^{32}P-labeled 28-mer primer complexed with a 90-mer DNA template by DNA pol δ in the presence or absence of PCNA and α-PCNA or Ref1 aptamer. Lanes: 1, 0; 2, 0.14; 3, 0.4; 4, 1.2; 5, 3.6; 6, 11; 7, 33; 8, 100; 9, 300; 10, 300; 11, 0; 12, 300 nM aptamer. Samples were separated on a 10% polyacrylamide gel containing 7 M urea. The signal was detected by autoradiography. (**D**) Signals from fully elongated 28-mer products presented on panel (C) quantified using ImageJ software. Values are normalized against the amount of full-length product in the absence of the α-PCNA aptamer. Results in (A), (B) and (D) are the means of three independent experiments. Results in (C) are representative. Error bars represent standard error. Asterisks indicate statistically significant differences: *$P = 0.01-0.05$; **$P = 0.001-0.01$; ***$P < 0.001$ (Tukey's test).

in the presence of PCNA (Figure 10A and B; lanes 11 and 12). Comparison of EMSA results obtained at 4°C (Figure 10A and B; lanes 9−12) and 32°C (Figure 11A and B; lanes 9−12) before glutaraldehyde treatment revealed an additional protective effect of PCNA against the exonuclease activity of DNA pol δ and ε with respect to the α-PCNA aptamer (similarly as observed in the previous experiment

(Figure 7)). Moreover, subsequent pull-down and immuno-precipitation experiments revealed that binding of PCNA to DNA pol enzymes was enhanced in the presence of the α-PCNA aptamer but not the Ref1 aptamer (Figure 12). Pull-down experiments with 30/90-mer primer-template DNA beads indicated that the α-PCNA aptamer but not the Ref1 aptamer could suppress the binding of DNA pol δ and
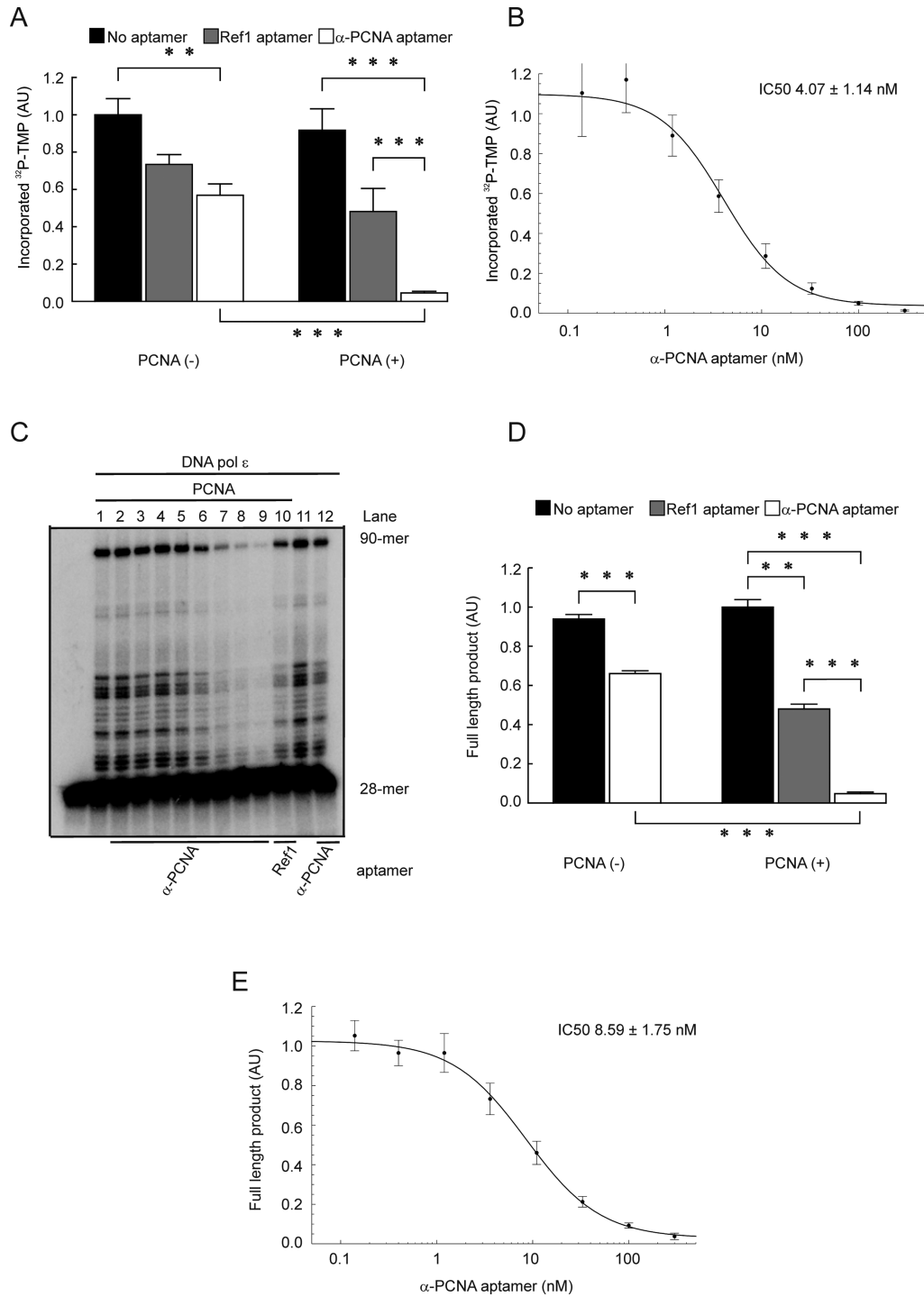
Figure 9. The impact of the α-PCNA aptamer on DNA pol ε activity in the presence or absence of PCNA. (**A**) Incorporation of ^{32}P-TMP into a dT/dA primer-template DNA by DNA pol ε in the presence or absence of PCNA and 100 nM α-PCNA or reference1 (Ref1) aptamer. The relative amount of ^{32}P-TMP incorporation was normalized against the mean amount of ^{32}P-TMP incorporated in the absence of PCNA and absence of aptamer. (**B**) Incorporation of ^{32}P-TMP into a dT/dA primer-template DNA by DNA pol ε in the presence of PCNA and increasing concentrations of α-PCNA aptamer (0.14, 0.4, 1.2, 3.6, 11.0, 33.0, 100 and 300 nM). Values are normalized against the amount of ^{32}P-TMP incorporated in the absence of the α-PCNA aptamer. (**C**) Extension of a 5′ ^{32}P-labeled 28-mer primer complexed with a 90-mer DNA template by DNA pol ε in the presence of α-PCNA or Ref1 aptamer. Lanes: 1, 0; 2, 0.14; 3, 0.4; 4, 1.2; 5, 3.6; 6, 11; 7, 33; 8, 100; 9, 300; 10, 300; 11, 0; 12, 300 nM aptamer. Samples were separated on a 10% polyacrylamide gel containing 7 M urea. The signal was detected by autoradiography. (**D**) Signals from fully elongated 28-mer products presented on panel (C) (lanes 11, 12, 1, 10 and 9) were quantified by ImageJ software. The relative amount of full-length product was normalized against the mean amount of the full-length product in the presence of PCNA and absence of aptamer. (**E**) The signal from the fully elongated 28-mer products (lanes 2–9) presented on panel (C). Values were normalized against the amount of full-length product in the absence of the α-PCNA aptamer. Results in (A), (B), (D) and (E) are the mean of three independent experiments. Error bars represent standard error. Asterisks indicate statistically significant differences: *$P = 0.01–0.05$; **$P = 0.001–0.01$; ***$P < 0.001$ (Tukey's test). Results in (C) are representative.
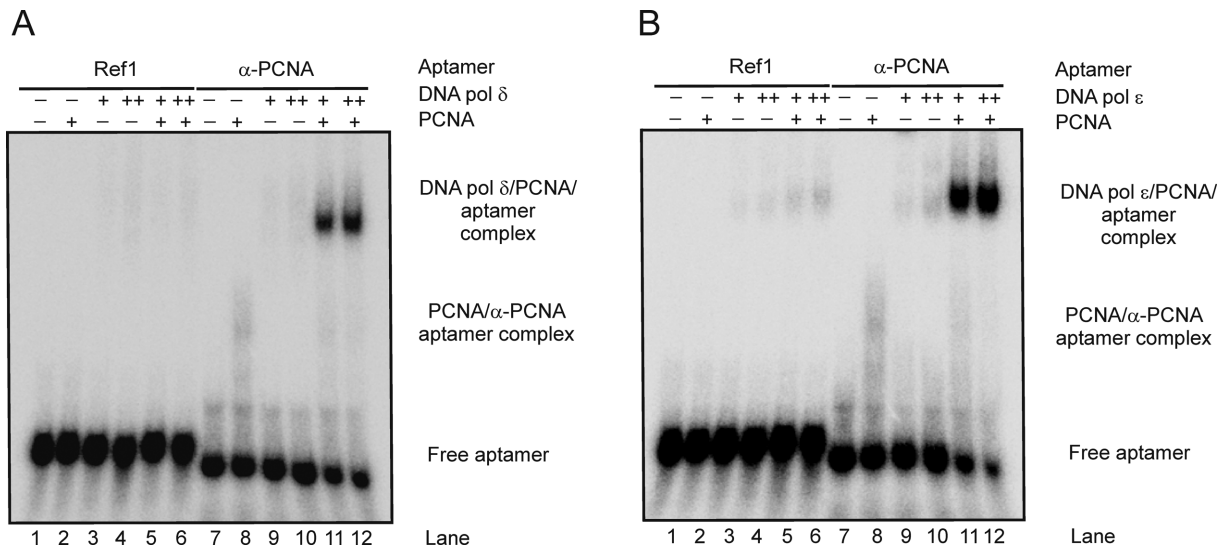
Figure 10. Analysis of α-PCNA aptamer, PCNA and DNA pol complex formation at 4°C by electrophoretic mobility shift assay (EMSA). A 10 fmol sample of 5′ ^{32}P-labeled Ref1 or α-PCNA aptamer, and 50 (+) or 100 (++) fmol of DNA pol δ (**A**) or DNA pol ε (**B**), were incubated with or without 1 pmol of PCNA on ice for 10 min. Next, the mixture was fixed with glutaraldehyde at 32°C, products were separated on a 5% polyacrylamide gel and the signal was detected by autoradiography. Results in (A) and (B) are representative.
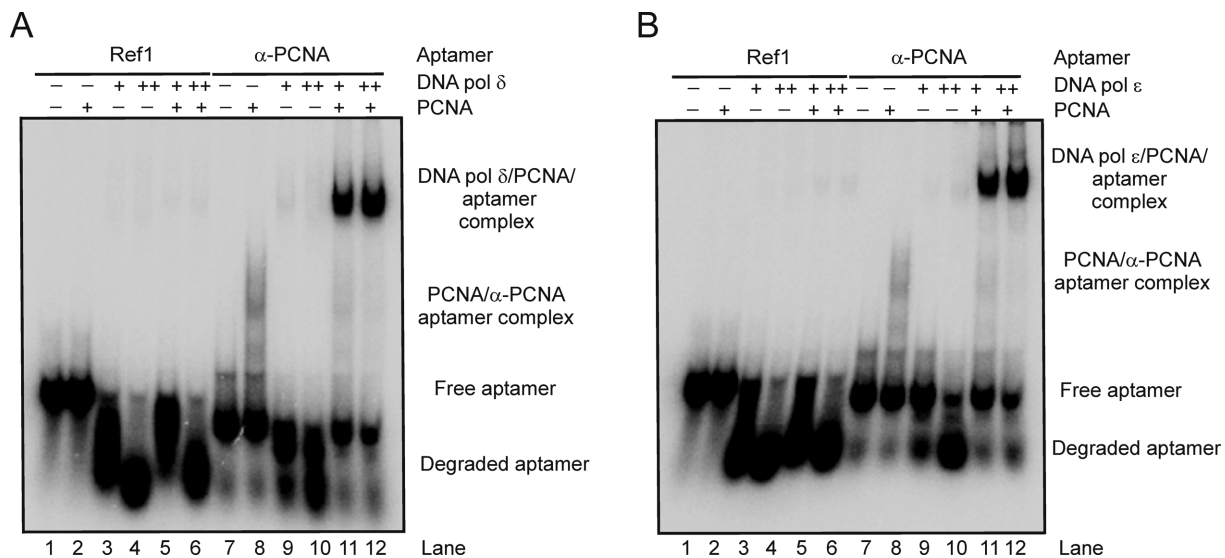
Figure 11. Analysis of α-PCNA aptamer, PCNA and DNA pol complex formation at 32°C by electrophoretic mobility shift assay (EMSA). A 10 fmol sample of 5′ ^{32}P-labeled Ref1 or α-PCNA aptamer, and 50 (+) or 100 (++) fmol of DNA pol δ (**A**) or DNA pol ε (**B**), were incubated with or without 1 pmol of PCNA at 32°C for 10 min before glutaraldehyde fixation. Products were separated on a 5% polyacrylamide gel, and the signal was detected by autoradiography. Results in (A) and (B) are representative.

ε to the 30/90-mer primer-template DNA in the presence of PCNA (Figure 13). Further comparison of the stability of α-PCNA aptamer/PCNA/DNA pol δ (Figure 14, lanes 8−10) and α-PCNA aptamer/PCNA/DNA pol ε (Figure 14, lanes 14−16) complexes, in the presence of excess 28/90-mer primer-template DNA, demonstrated that only the latter could be outcompeted by excess primer-template DNA. This suggests that the complex containing DNA pol δ is more stable than the complex with DNA pol ε.

DISCUSSION

PCNA is one of several proteins that work together at the heart of the DNA replication machinery. PCNA is considered a non-oncogenic target for anti-cancer therapy (15–17), and molecules that inhibit or otherwise control PCNA function might prove useful in the development of novel cancer treatments. Previous *in vitro* data showed that short peptides can control PCNA function, such as PIP-box (32) and APIM motif-based peptides (13,33) that block interactions between PCNA and proteins containing these motifs. Moreover the Y211F peptide blocks phosphorylation of PCNA tyrosine 211 (19). Other experiments demonstrated that the T3 hormone triiodothyronine and its analog T2AA (the amino alcohol of T3 lacking hor-

A

B

Figure 12. The impact of the α-PCNA aptamer on the PCNA/DNA pol interaction. An 800 fmol sample of DNA pol δ (**A**) and 1300 fmol of DNA pol ε (**B**) were bound to Ni-NTA and agarose-protein anti-FLAG M2 affinity beads, respectively. Beads were incubated with 4 pmol of PCNA in the presence and absence of 5 pmol of reference1 (Ref1) or α-PCNA aptamer. After incubation, unbound protein was removed by washing, and proteins bound to beads were denatured, separated by 10% SDS-PAGE and subjected to western blotting. DNA pol δ and ε and PCNA were detected using anti-p125 and -p261 antibodies, and anti-human PCNA polyclonal serum, respectively. The presented results are representative.

mone activity) can block the PCNA/PIP-box interaction (34). Moreover, T2AA and its analogs can suppress translesion DNA synthesis (34), which allows the DNA replication machinery to replicate past DNA lesions such as pirymidine dimers or apurinic/apyrimidinic sites (35,36). Another small molecule, PCNA-I1, inhibits the association of PCNA with chromatin (37).

In the early stages of the present work, after identifying the A1 aptamer, we found that the affinity of the A1 aptamer variant truncated at the 5′ end towards PCNA was significantly reduced (Figure 1). This indicated that the 5′ region might be involved in PCNA binding and/or be crucial for adoption of the correct aptamer structure. By contrast, the 3′ end of the A1 aptamer was superfluous, and deletion did not affect aptamer activity. Moreover, the affinity of the α-PCNA aptamer (A1 aptamer variant truncated at the 3′ end) toward PCNA was higher than that of the full-length A1 aptamer. This indicates that the 30 nt at the 3′ end of the A1 aptamer may sterically hinder and thereby prevent an optimal fit between the aptamer and PCNA. The secondary structure of the modeled α-PCNA aptamer, which

mimics the DNA replication fork (Figure 2), indicates that the central cavity of the PCNA ring is probably located on the dsDNA fragment close to the dsDNA/ssDNA interface. This is unsurprising because, during DNA replication, PCNA is loaded near the primer-template DNA junction to coordinate replicative DNA pol enzymes (38). Moreover, an α-PCNA aptamer blocked at the 5′ terminus by streptavidin (Figure 1), which is unable to enter the cavity of the PCNA ring, could still interact with PCNA. This indicates that postulated localization of PCNA on the dsDNA fragment of the α-PCNA aptamer is not essential for interaction between the α-PCNA aptamer and PCNA, and the exact nature of the specific interaction must involve other parts. Unfortunately, our attempts to solve the crystal structure of the α-PCNA aptamer/PCNA complex were unsuccessful; hence we employed CD analysis, which revealed less correctly folded α-PCNA aptamer at 37°C than at 25°C. Perhaps this effect could be eliminated if the aptamer selection process was performed at 37°C. Moreover, the CD spectrum of the α-PCNA aptamer was typical of B-form DNA, and CD analysis indicated that, during complex formation, the structure of the α-PCNA aptamer became altered, but the structure of PCNA did not change. This is understandable given the stable and highly ordered structure of the PCNA trimer under the experimental conditions employed. To further investigate the properties of the α-PCNA aptamer/PCNA complex, we determined the K_D value using pull-down assays and ITC, and K_D values obtained by both techniques were in the μM range. However, the K_D value from pull-down assays was over 2-fold higher than the value from ITC (5.1 μM versus 2.0 μM; Figures 3 and 4,), which is insignificant in the context of understanding the impact of the α-PCNA aptamer on DNA replication. This apparent discrepancy possibly results from differences in the accuracy of the two methods. Although we cannot exclude the trace leakage of biotinylated aptamer from streptavidin during the experiment, the strong binding between streptavidin and biotin ($K_D \sim 10^{-14}$ M) (39) makes this unlikely to have a significant impact on the measured K_D value. Interestingly, the stoichiometry of the α-PCNA aptamer/PCNA (trimer) complex calculated from ITC data was 1.44. The fractional value could be due to inaccurate ss-DNA and protein concentration determinations.

To test the impact of the α-PCNA aptamer on the activity of DNA pol δ and ε, we first checked whether the DNA pol enzymes could extend the 3′ end of the α-PCNA aptamer, but the α-PCNA aptamer was unable to sufficiently mimic the primer-template DNA structure (Figure 7). Moreover, protection of the α-PCNA aptamer by PCNA against the exonucleolytic activity of DNA pol δ and ε was not surprising, since the α-PCNA aptamer secondary/tertiary structure formed upon PCNA binding was presumably largely inaccessible to the DNA pol regions exhibiting exonuclease activity. When we tested the impact of the α-PCNA aptamer and PCNA on DNA synthesis by DNA pol δ and ε, several unexpected features were observed. First, the α-PCNA aptamer inhibited both DNA pol enzymes at nM concentrations in the presence of PCNA (Figures 8 and 9). The measured IC50 values of the α-PCNA aptamer for both DNA pol enzymes (nM) were three orders of magnitude lower than the K_D (μM) between the α-PCNA aptamer and
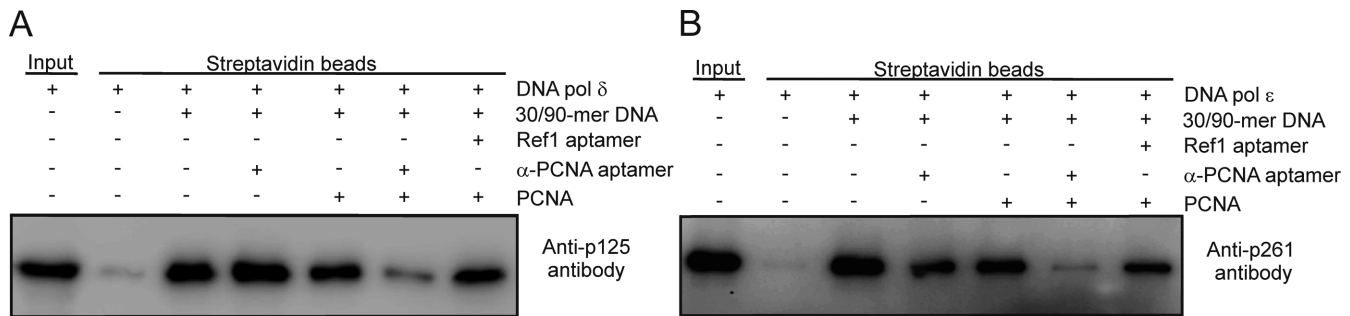
Figure 13. The impact of the α-PCNA aptamer and PCNA on the 30/90-mer primer-template DNA/DNA pol δ or ε complex. A 300 fmol sample of DNA pol δ (**A**) and 400 fmol of DNA pol ε (**B**) were incubated with 1 pmol of 30/90-mer primer-template DNA immobilized on streptavidin-agarose beads in buffer with or without 1 pmol of PCNA, and with 500 fmol (**A**) or 250 fmol (**B**) of reference1 (Ref1) or α-PCNA aptamer. After incubation, beads were washed, and bound protein was denatured, separated by 10% SDS-PAGE and subjected to western blotting. DNA pol δ and ε were detected using anti-p125 and -p261 antibodies, respectively. The presented results are representative.
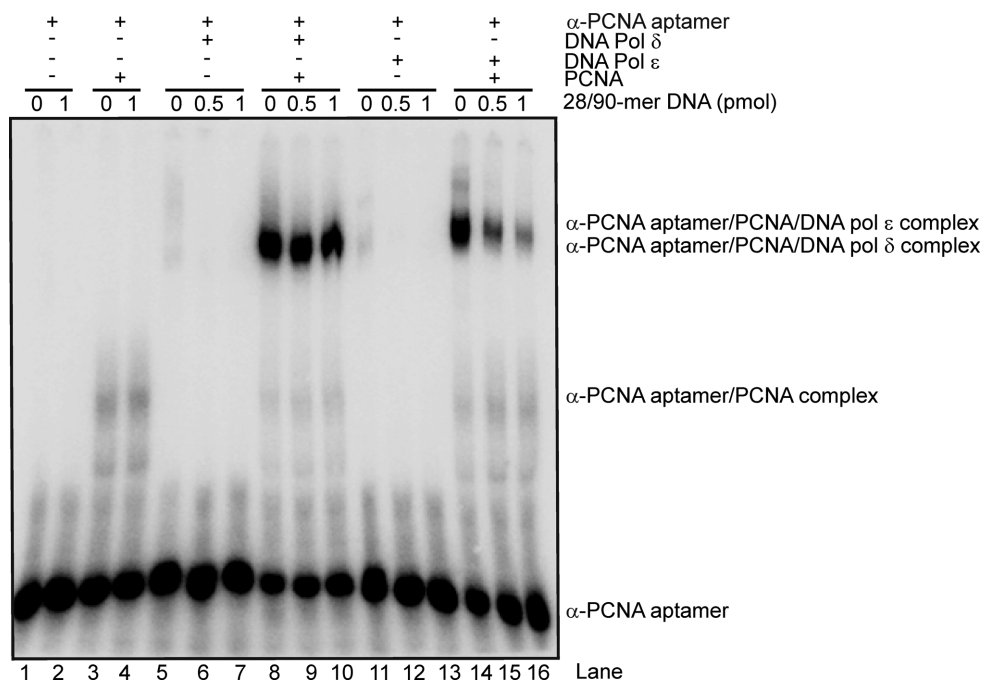

Figure 14. Stability of the α-PCNA aptamer/PCNA/DNA pol δ and α-PCNA aptamer/PCNA/DNA pol ε complexes in the presence of 28/90-mer primer-template DNA. A 10 fmol sample of 5′ ^{32}P-labeled α-PCNA aptamer, and 50 fmol of DNA pol δ or DNA pol ε, were incubated with or without 1 pmol of PCNA and 0, 0.5 or 1 pmol of 28/90-mer primer-template DNA at 4°C for 10 min before glutaraldehyde fixation. Products were separated on a 5% polyacrylamide gel, and the signal was detected by autoradiography. The presented results are representative.

PCNA measured by pull-down assays and ITC. In the absence of PCNA, the α-PCNA aptamer did not affect DNA synthesis by DNA pol δ (Figure 8A and C), suggesting that the aptamer did not block/bind DNA pol δ directly. In the case of DNA pol ε, DNA synthesis in the absence of PCNA was slightly inhibited by 300 nM α-PCNA or Ref1 aptamers (Figure 9A). We concluded that this was non-specific inhibition of DNA pol ε by addition of excess non-primer-template DNA. Similar effect was previously described for yeast DNA pol ε, which was shown to bind ssDNA as well as dsDNA in the absence of PCNA, and ssDNA blocked the activity of yeast DNA pol ε in a non-specific manner (40). Moreover, DNA pol activity assays revealed that addition of both the α-PCNA aptamer and PCNA to DNA pol δ or ε reduced DNA synthesis levels to below those in the absence

of PCNA (Figures 8A and 9A white bars - comparison between PCNA (−) and (+)). If the α-PCNA aptamer simply blocked the formation of PCNA/DNA pol complexes, DNA synthesis with saturating α-PCNA aptamer would be comparable to that without PCNA, but not lower. Given that (i) a stable complex between calf thymus DNA pol δ and dsDNA containing a protruding 5′ end forms in the presence of PCNA (41), (ii) the α-PCNA aptamer in the modeled non-functional primer-template DNA junction-like structure has a protruding 5′ end (Figure 2) and (iii) DNA pol activity assays yielded a nM IC50 of the α-PCNA aptamer (Figures 8 and 9), we concluded that the α-PCNA aptamer, PCNA and DNA pol enzymes potentially form novel α-PCNA aptamer/PCNA/DNA pol complexes that are hardly accessible to the primer-template DNA.
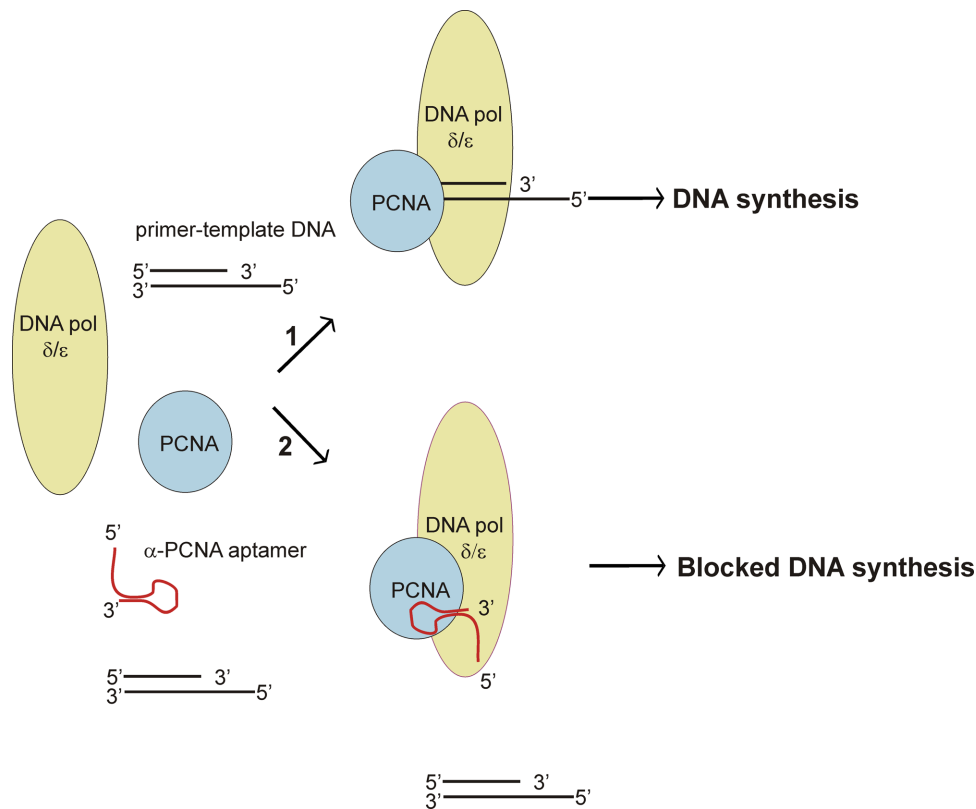
Figure 15. Putative model of α-PCNA aptamer/PCNA complex-dependent inhibition of DNA replication. The α-PCNA aptamer and primer-template DNA appear to compete for binding to the PCNA/DNA pol δ/ε complex. The α-PCNA aptamer-specific inhibition of DNA pol is dependent on the presence of PCNA. (**1**) In the absence of the α-PCNA aptamer, the primer-template DNA forms a tri-molecular complex with PCNA and DNA pol δ or ε, and replication of the DNA template is undisturbed; (**2**) In the presence of the α-PCNA aptamer, rather than primer-template DNA/PCNA/DNA pol δ or ε complex formation, assembly of the α-PCNA aptamer/PCNA/DNA pol δ or ε complex is favored. The α-PCNA aptamer/PCNA/DNA pol δ or ε complex blocks formation of a primer-template DNA/PCNA/DNA pol δ/ε complex, thereby preventing template DNA replication.

Based on the results of DNA pol δ/ε activity assays and ITC experiments, we built a preliminary model of the α-PCNA aptamer/PCNA complex-dependent mechanism of DNA pol δ/ε activity inhibition. Given that (i) the α-PCNA aptamer inhibited the activity of DNA pol δ only in the presence of PCNA (Figure 8), (ii) the α-PCNA aptamer effectively inhibited the activity of DNA pol δ/ε at low nM concentrations (e.g. 10 nM) in the presence of excess PCNA (200 nM) and DNA template (160 nM; Figures 8 and 9), despite the fact that the α-PCNA aptamer/PCNA complex K_D value was in the μM range (Figure 5), (iii) the strength of the α-PCNA aptamer-dependent inhibition of DNA pol δ/ε activity was enhanced in the presence of PCNA (Figures 8 and 9) and (iv) excess PCNA (200 nM) did not affect the activity of DNA pol δ in the presence of stoichiometric concentrations of α-PCNA aptamer (10 nM) and DNA pol δ (10 nM), we concluded that the determined nM IC50 value reflects a K_D in the nM range or lower for the association of the bi-molecular α-PCNA aptamer/PCNA complex with DNA pol enzymes. Presumably, the α-PCNA aptamer/PCNA/DNA pol complex K_D must be much lower than that of the α-PCNA aptamer/PCNA (Figures 10 and 11) and PCNA/DNA pol δ/ε complexes. Unfortunately, we could not directly measure this value using ITC due to technical limitations (insufficient production of DNA pol enzymes). This raises the important question: which factors are responsible for the increased stability of the tri-molecular complex (α-PCNA aptamer/PCNA/DNA pol) compared with the bi-molecular complexes (α-PCNA aptamer/PCNA and PCNA/DNA pol)? We cannot exclude the possibility that a change in the α-PCNA aptamer structure may stabilize the α-PCNA aptamer/PCNA/DNA pol tri-molecular complex. Another possibility is that aptamer structural changes are not significant and the higher stability of the tri-molecular complex is a result of additional favorable interactions between the components of the complex, i.e. α-PCNA aptamer/DNA pol, α-PCNA aptamer/PCNA and PCNA/DNA pol (e.g. via the PIP-box motif). In this case, the α-PCNA aptamer could mimic a non-functional DNA replication fork structure.

To verify our hypothesis that a tri-molecular complex is formed, additional experiments were conducted to investigate (i) the formation of the α-PCNA aptamer/PCNA/DNA pol complex (Figures 10 and 11), (ii) the impact of the α-PCNA aptamer on PCNA/DNA pol complex stability (Figure 12), (iii) the impact of the α-PCNA aptamer and/or PCNA on primer-template DNA/DNA pol complex stability (Figure 13) and (iv) the impact of primer-template DNA on α-PCNA aptamer/PCNA/DNA pol complex stability (Figure 14). The results presented in Figures 10 and 11 revealed a poor

signal from the α-PCNA aptamer/PCNA bi-molecular complex, consistent with the K_D value determined by ITC (Figure 4) and supporting our calculation. Moreover, these results confirmed our hypothesis that the α-PCNA aptamer formed a complex with PCNA/DNA pol, but it did not block the formation of complexes composed of PCNA and DNA pol enzymes involved in DNA replication (previously shown to act in complex with PCNA during DNA replication) (7). Rather, the α-PCNA aptamer strengthened the affinity between PCNA and DNA pol enzymes (Figure 12). Subsequent data from DNA pol activity assays (Figures 8 and 9) and EMSA (Figure 14) indicated the higher stability of the α-PCNA aptamer/PCNA/DNA pol δ complex relative to the α-PCNA aptamer/PCNA/DNA pol ε complex. This conclusion was based on the fact that a 50- to 100-fold higher amount of 28/90-mer primer-template DNA was unable to displace the α-PCNA aptamer from the α-PCNA aptamer/PCNA/DNA pol δ complex (Figure 14). This is particularly interesting in the context of DNA replication, and suggests that the α-PCNA aptamer might block DNA replication, resulting in uncoordinated leading and lagging DNA strand replication. In principle, an appropriate amount of α-PCNA aptamer could completely block replication of the leading DNA strand, mediated by DNA pol ε but not lagging DNA strand, mediated by DNA pol δ. In the future, it would be interesting to develop an aptamer with a significantly lower affinity for PCNA/DNA pol δ but an undisturbed affinity for PCNA/DNA pol ε, or *vice versa*. Moreover, in the context of DNA replication, it would be especially interesting to analyze the impact of the α-PCNA aptamer on other DNA pol enzymes that cooperate with PCNA, such as those belonging to the Y-family (e.g. DNA pol η, ι, κ or Rev1), to assess whether, and if so how, the α-PCNA aptamer affects their activity.

CONCLUSION

Given the potential of PCNA as a non-oncogenic anti-cancer therapeutic target (16), in this study we developed and characterized the α-PCNA aptamer. Based on the results, we propose that the α-PCNA aptamer, which undergoes a change in secondary structure upon binding to PCNA, blocks replication of the DNA template by forming an α-PCNA aptamer/PCNA/DNA pol complex that is unable to bind the primer-template DNA (Figure 15). The proposed model of the α-PCNA aptamer-dependent inhibition of DNA replication differs substantially from those previously reported for molecules controlling PCNA functions (13,18,19,32). Finally, although our experiments did not indicate that the α-PCNA aptamer inhibits the formation of complexes between PCNA and human DNA pol enzymes, we cannot exclude this possibility for other proteins that use PCNA as a sliding platform (42,43).

SUPPLEMENTARY DATA

Supplementary Data are available at NAR Online.

ACKNOWLEDGEMENTS

We thank Agnieszka Banaś, Justyna Łabuz and Piotr Zgłobicki for comments on this manuscript.

REFERENCES

1. Strzalka,W. and Ziemienowicz,A. (2011) Proliferating cell nuclear antigen (PCNA): a key factor in DNA replication and cell cycle regulation. *Ann. Bot.*, **107**, 1127–1140.
2. Witko-Sarsat,V., Mocek,J., Bouayad,D., Tamassia,N., Ribeil,J.A., Candalh,C., Davezac,N., Reuter,N., Mouthon,L., Hermine,O. *et al.* (2010) Proliferating cell nuclear antigen acts as a cytoplasmic platform controlling human neutrophil survival. *J. Exp. Med.*, **207**, 2631–2645.
3. Rosental,B., Brusilovsky,M., Hadad,U., Oz,D., Appel,M.Y., Afergan,F., Yossef,R., Rosenberg,L.A., Aharoni,A., Cerwenka,A. *et al.* (2011) Proliferating cell nuclear antigen is a novel inhibitory ligand for the natural cytotoxicity receptor NKp44. *J. Immunol.*, **187**, 5693–5702.
4. Brand,S.R., Bernstein,R.M. and Mathews,M.B. (1994) Trimeric structure of human proliferating cell nuclear antigen. Implications for enzymatic function and autoantibody recognition. *J. Immunol.*, **153**, 3070–3078.
5. Gulbis,J.M., Kelman,Z., Hurwitz,J., O'Donnell,M. and Kuriyan,J. (1996) Structure of the C-terminal region of p21(WAF1/CIP1) complexed with human PCNA. *Cell*, **87**, 297–306.
6. Moldovan,G.L., Pfander,B. and Jentsch,S. (2007) PCNA, the maestro of the replication fork. *Cell*, **129**, 665–679.
7. Maga,G. and Hubscher,U. (2003) Proliferating cell nuclear antigen (PCNA): a dancer with many partners. *J. Cell Sci.*, **116**, 3051–3060.
8. Warbrick,E. (2000) The puzzle of PCNA's many partners. *Bioessays*, **22**, 997–1006.
9. Wu,X., Li,J., Li,X., Hsieh,C.L., Burgers,P.M. and Lieber,M.R. (1996) Processing of branched DNA intermediates by a complex of human FEN-1 and PCNA. *Nucleic Acids Res.*, **24**, 2036–2043.
10. Tom,S., Henricksen,L.A., Park,M.S. and Bambara,R.A. (2001) DNA ligase I and proliferating cell nuclear antigen form a functional complex. *J. Biol. Chem.*, **276**, 24817–24825.
11. Jonsson,Z.O. and Hubscher,U. (1997) Proliferating cell nuclear antigen: more than a clamp for DNA polymerases. *Bioessays*, **19**, 967–975.
12. Xu,H., Zhang,P., Liu,L. and Lee,M.Y. (2001) A novel PCNA-binding motif identified by the panning of a random peptide display library. *Biochemistry*, **40**, 4512–4520.
13. Gilljam,K.M., Feyzi,E., Aas,P.A., Sousa,M.M., Muller,R., Vagbo,C.B., Catterall,T.C., Liabakk,N.B., Slupphaug,G., Drablos,F. *et al.* (2009) Identification of a novel, widespread, and functionally important PCNA-binding motif. *J. Cell Biol.*, **186**, 645–654.
14. Mailand,N., Gibbs-Seymour,I. and Bekker-Jensen,S. (2013) Regulation of PCNA-protein interactions for genome stability. *Nat. Rev. Mol. Cell Biol.*, **14**, 269–282.
15. Nagel,R., Semenova,E.A. and Berns,A. (2016) Drugging the addict: non-oncogene addiction as a target for cancer therapy. *EMBO Rep.*, **17**, 1516–1531.
16. Stoimenov,I. and Helleday,T. (2009) PCNA on the crossroad of cancer. *Biochem. Soc. Trans.*, **37**, 605–613.

17. Wang,S.C. (2014) PCNA: a silent housekeeper or a potential therapeutic target? *Trends Pharmacol. Sci.*, **35**, 178–186.
18. Punchihewa,C., Inoue,A., Hishiki,A., Fujikawa,Y., Connelly,M., Evison,B., Shao,Y., Heath,R., Kuraoka,I., Rodrigues,P. *et al.* (2012) Identification of small molecule proliferating cell nuclear antigen (PCNA) inhibitor that disrupts interactions with PIP-box proteins and inhibits DNA replication. *J. Biol. Chem.*, **287**, 14289–14300.
19. Zhao,H., Lo,Y.H., Ma,L., Waltz,S.E., Gray,J.K., Hung,M.C. and Wang,S.C. (2011) Targeting tyrosine phosphorylation of PCNA inhibits prostate cancer growth. *Mol. Cancer Ther.*, **10**, 29–36.
20. Yang,X., Wang,H., Beasley,D.W., Volk,D.E., Zhao,X., Luxon,B.A., Lomas,L.O., Herzog,N.K., Aronson,J.F., Barrett,A.D. *et al.* (2006) Selection of thioaptamers for diagnostics and therapeutics. *Ann. N.Y. Acad. Sci.*, **1082**, 116–119.
21. Knudsen,S.M., Robertson,M.P. and Ellington,A.D. (2002) In vitro selection using modified or unnatural nucleotides. *Curr. Protoc. Nucleic Acid. Chem.*. doi: 10.1002/0471142700.nc0906s07.
22. Xing,H., Tang,L., Yang,X., Hwang,K., Wang,W., Yin,Q., Wong,N.Y., Dobrucki,L.W., Yasui,N., Katzenellenbogen,J.A. *et al.* (2013) Selective delivery of an anticancer drug with aptamer-functionalized liposomes to breast cancer cells in vitro and in vivo. *J. Mater. Chem. B. Mater. Biol. Med.*, **1**, 5288–5297.
23. Ellington,A.D. and Szostak,J.W. (1990) In vitro selection of RNA molecules that bind specific ligands. *Nature*, **346**, 818–822.
24. Tuerk,C. and Gold,L. (1990) Systematic evolution of ligands by exponential enrichment: RNA ligands to bacteriophage T4 DNA polymerase. *Science*, **249**, 505–510.
25. Shiomi,Y., Masutani,C., Hanaoka,F., Kimura,H. and Tsurimoto,T. (2007) A second proliferating cell nuclear antigen loader complex, Ctf18-replication factor C, stimulates DNA polymerase eta activity. *J. Biol. Chem.*, **282**, 20906–20914.
26. Murakami,T., Takano,R., Takeo,S., Taniguchi,R., Ogawa,K., Ohashi,E. and Tsurimoto,T. (2010) Stable interaction between the human proliferating cell nuclear antigen loader complex Ctf18-replication factor C (RFC) and DNA polymerase {epsilon} is mediated by the cohesion-specific subunits, Ctf18, Dcc1, and Ctf8. *J. Biol. Chem.*, **285**, 34608–34615.
27. Narita,T., Tsurimoto,T., Yamamoto,J., Nishihara,K., Ogawa,K., Ohashi,E., Evans,T., Iwai,S., Takeda,S. and Hirota,K. (2010) Human replicative DNA polymerase delta can bypass T-T (6-4) ultraviolet photoproducts on template strands. *Genes Cells*, **15**, 1228–1239.
28. Kowalska,E., Bartnicki,F., Pels,K. and Strzalka,W. (2014) The impact of immobilized metal affinity chromatography (IMAC) resins on DNA aptamer selection. *Anal. Bioanal. Chem.*, **406**, 5495–5499.
29. Bartnicki,F., Kowalska,E., Pels,K. and Strzalka,W. (2015) Imidazole-free purification of His3-tagged recombinant proteins using ssDNA aptamer-based affinity chromatography. *J. Chromatogr. A*, **1418**, 130–139.
30. Bartnicki,F., Bonarek,P., Kowalska,E. and Strzalka,W. (2017) The Argi system: one-step purification of proteins tagged with arginine-rich cell-penetrating peptides. *Sci. Rep.*, **7**, 2619.
31. Zuker,M. (2003) Mfold web server for nucleic acid folding and hybridization prediction. *Nucleic Acids Res.*, **31**, 3406–3415.
32. Warbrick,E., Lane,D.P., Glover,D.M. and Cox,L.S. (1995) A small peptide inhibitor of DNA replication defines the site of interaction between the cyclin-dependent kinase inhibitor p21WAF1 and proliferating cell nuclear antigen. *Curr. Biol.*, **5**, 275–282.
33. Muller,R., Misund,K., Holien,T., Bachke,S., Gilljam,K.M., Vatsveen,T.K., Ro,T.B., Bellacchio,E., Sundan,A. and Otterlei,M. (2013) Targeting proliferating cell nuclear antigen and its protein interactions induces apoptosis in multiple myeloma cells. *PLoS One*, **8**, e70430.
34. Actis,M., Inoue,A., Evison,B., Perry,S., Punchihewa,C. and Fujii,N. (2013) Small molecule inhibitors of PCNA/PIP-box interaction suppress translesion DNA synthesis. *Bioorg. Med. Chem.*, **21**, 1972–1977.
35. Lange,S.S., Takata,K. and Wood,R.D. (2011) DNA polymerases and cancer. *Nat. Rev. Cancer*, **11**, 96–110.
36. Goodman,M.F. and Woodgate,R. (2013) Translesion DNA polymerases. *Cold Spring Harb. Perspect. Biol.*, **5**, a010363.
37. Tan,Z., Wortman,M., Dillehay,K.L., Seibel,W.L., Evelyn,C.R., Smith,S.J., Malkas,L.H., Zheng,Y., Lu,S. and Dong,Z. (2012) Small-molecule targeting of proliferating cell nuclear antigen chromatin association inhibits tumor cell growth. *Mol. Pharmacol.*, **81**, 811–819.
38. Tsurimoto,T. and Stillman,B. (1991) Replication factors required for SV40 DNA replication in vitro. I. DNA structure-specific recognition of a primer-template junction by eukaryotic DNA polymerases and their accessory proteins. *J. Biol. Chem.*, **266**, 1950–1960.
39. Green,N.M. (1990) Avidin and streptavidin. *Methods Enzymol.*, **184**, 51–67.
40. Ng,L., McConnell,M., Tan,C.K., Downey,K.M. and Fisher,P.A. (1993) Interaction of DNA polymerase delta, proliferating cell nuclear antigen, and synthetic oligonucleotide template-primers. Analysis by polyacrylamide gel electrophoresis-band mobility shift assay. *J. Biol. Chem.*, **268**, 13571–13576.
41. Tsubota,T., Maki,S., Kubota,H., Sugino,A. and Maki,H. (2003) Double-stranded DNA binding properties of Saccharomyces cerevisiae DNA polymerase epsilon and of the Dpb3p-Dpb4p subassembly. *Genes Cells*, **8**, 873–888.
42. Sporbert,A., Domaing,P., Leonhardt,H. and Cardoso,M.C. (2005) PCNA acts as a stationary loading platform for transiently interacting Okazaki fragment maturation proteins. *Nucleic Acids Res.*, **33**, 3521–3528.
43. Arias,E.E. and Walter,J.C. (2006) PCNA functions as a molecular platform to trigger Cdt1 destruction and prevent re-replication. *Nat. Cell Biol.*, **8**, 84–90.